Shaker Potassium Channel Gating II: Transitions in the Activation Pathway

WILLIAM N. ZAGOTTA, TOSHINORI HOSHI, JEREMY DITTMAN, and RICHARD W. ALDRICH

From the Department of Molecular and Cellular Physiology, Howard Hughes Medical Institute, Stanford University School of Medicine, Stanford, California 94305

ABSTRACT Voltage-dependent gating behavior of *Shaker* potassium channels without N-type inactivation (ShBΔ6-46) expressed in *Xenopus* oocytes was studied. The voltage dependence of the steady-state open probability indicated that the activation process involves the movement of the equivalent of 12–16 electronic charges across the membrane. The sigmoidal kinetics of the activation process, which is maintained at depolarized voltages up to at least +100 mV indicate the presence of at least five sequential conformational changes before opening. The voltage dependence of the gating charge movement suggested that each elementary transition involves 3.5 electronic charges. The voltage dependence of the forward opening rate, as estimated by the single-channel first latency distribution, the final phase of the macroscopic ionic current activation, the ionic current reactivation and the ON gating current time course, showed movement of the equivalent of 0.3 to 0.5 electronic charges were associated with a large number of the activation transitions. The equivalent charge movement of 1.1 electronic charges was associated with the closing conformational change. The results were generally consistent with models involving a number of independent and identical transitions with a major exception that the first closing transition is slower than expected as indicated by tail current and OFF gating charge measurements.

INTRODUCTION

Like other voltage-gated channels, ShBΔ6-46 channels activate with a sigmoidal time course in response to a depolarizing voltage step (Hoshi, Zagotta, and Aldrich, 1994). The sigmoidal character of the macroscopic activation kinetics indicates that the

Address correspondence to Richard W. Aldrich, Department of Molecular and Cellular Physiology, Stanford University School of Medicine, Stanford, California 94305-5426.

Dr. Zagotta's present address is Department of Physiology and Biophysics, SJ-40, University of Washington, Seattle, WA 98195.

Dr. Hoshi's present address is Department of Physiology and Biophysics, University of Iowa, Iowa City, IA 52242-1109.

Dr. Dittman's present address is Harvard Medical School, Boston, MA 02115.

J. GEN. PHYSIOL. © The Rockefeller University Press · 0022-1295/94/02/0279/41 $2.00
Volume 103 February 1994 279–319

channel must undergo a number of conformational transitions before opening. The overall time course of these transitions is appreciably voltage dependent indicating that there must be an intrinsic charge movement in the channel protein associated with at least some of the conformational changes. In addition, some of the conformational transitions may not alter the charge distribution of the channel protein in the membrane electric field and would therefore be unaffected by changes in the transmembrane voltage. The kinetic behavior of the channel ultimately depends on the rates and voltage dependencies of all of these transitions.

The analysis of the single-channel currents has provided only limited insight into the nature of these conformational changes. As shown in the previous paper (Hoshi et al., 1994), most of the closing transitions, particularly at depolarized voltages, are to closed states not directly in the activation pathway. Furthermore it is difficult to obtain enough single-channel events to accurately measure the slower components in the closed time distributions at hyperpolarized voltages. The distributions of the latencies to first opening have time courses that are virtually identical to the time courses of the probability of being open at depolarized voltages (Hoshi et al., 1994). Therefore, the macroscopic activation time course in these channels provides a reasonable estimate of the time course of the conformational changes involved in activation at depolarized voltages. At hyperpolarized voltages where the rate constant for the deactivation transition becomes appreciable, the macroscopic activation time course and first latency distributions would not be expected to superimpose.

The activation process in voltage-dependent potassium channels has been extensively studied by many investigators (Hille, 1992). These investigations utilized many different types of macroscopic, single-channel, and gating current experiments to explore different aspects of the activation process. However, most of these experiments were done on channels from different cells or different species, making comparison of the results difficult. Furthermore, because of the channel density and the presence of other endogenous currents, most of these preparations are not adequate for doing all of the different types of experiments. The exogenous expression of *Shaker* channels in *Xenopus* oocytes has alleviated these problems. The oocytes do not contain an appreciable level of endogenous voltage-dependent channels so virtually all of the ionic and gating currents arise from a pure population of Shaker channels. In addition, by varying the amount of RNA injected into the oocyte, we can record single-channel currents, macroscopic currents, and gating currents all in cell-free patches in the same preparation. This has permitted us to consider the results from a number of different types of experiments done in the same preparation and in channels whose primary structure can be manipulated.

In this paper we will analyze the steady state and kinetic behavior of the *Shaker* channel to identify some general properties of the activation gating mechanism. We will derive many of these properties from a comparison of the data to the predictions of a mechanism involving multiple transitions which will be modeled as time-homogeneous Markov processes. In the following paper (Zagotta, Hoshi, and Aldrich, 1994), we will consider a number of specific kinetic models to account for these properties.

MATERIALS AND METHODS

Experiments were carried out and the data analyzed as described in the preceding paper (Hoshi et al., 1994).

Ionic Currents

Unless otherwise noted, the macroscopic currents were recorded in the inside-out configuration with borosilicate pipettes with typical resistances of 0.5 to 1.5 MΩ. The external solution contained (in millimolar): 140 NaCl, 6 $MgCl_2$, 2 KCl, 10 HEPES (NaOH), pH 7.1. The internal solution contained (in millimolar): 140 KCl, 2 $MgCl_2$, 11 EGTA, 1 $CaCl_2$, 10 HEPES (*N*-methylglucamine [NMG]), pH 7.2; free [Ca^{2+}] is calculated to be ~10 nM. Other solutions used are described in the legends. Series resistance compensation was not used. The estimated voltage error caused by the uncompensated series resistance was <3 mV. Typically, the capacitative transients settled within <30 μs before filtering. Linear leak and capacitative currents were subtracted either by scaling the average current response to 15 to 20 mV voltage steps or by a P/4 or P/6 procedure with the typical leak holding voltage of −110 mV. We found that the macroscopic currents occasionally reversed at more positive voltages than expected from the Nernst equation prediction or from the reversal voltage estimated from the single-channel current-voltage relationship ($i[V]$). This observation is consistent with the accumulation of K^+ in the extracellular space. We routinely checked the reversal voltages of the recorded currents and discarded the data if noticeable inward tail currents were seen at −90 mV.

Gating Currents

Gating currents were measured in the absence of any permeant ions. Na^+ and K^+ ions were replaced with *N*-methylglucamine (NMG^+). The external solution contained (in millimolar): 140 NMGCl, 6 $MgCl_2$, 5 HEPES (HCl), pH 7.1. The intracellular solution contained (in millimolar): 140 NMGCl, 11 EGTA, 2 $MgCl_2$, 1 $CaCl_2$, 10 HEPES (HCl), pH 7.2. Ohmic capacitative and leak currents are subtracted in the following three different ways; (*a*) P/4 or P/6 protocol from a leak holding voltage ≤ −110 mV. (*b*) P/−4 or P/−6 protocol from a leak holding voltage ≤ −110 mV. (*c*) P/4 or P/6 protocol with a leak holding voltage of +50 mV. With the P/4 or P/−4 procedure with a negative leak holding voltage, the initial phases of the OFF gating currents were often outward and followed by large inward currents. These OFF currents are at least in part artifacts of the leak subtraction procedures (Stuhmer, Conti, Stocker, Pongs, and Heinemann, 1991) and could be eliminated by using a P/4 protocol with a very positive leak holding voltage (+50 mV) or by additional leak subtraction procedures that consider the charge movements near the leak holding voltage (Stuhmer et al., 1991). The ON transients are not markedly affected by these different subtraction procedures. Kinetics of the gating currents with different amplitudes (50 to 300 pA at +50 mV) were very similar. All the gating currents presented are recorded using the P/4 protocol with the leak holding voltage of +50 mV.

The macroscopic currents are corrected for the eight pole Bessel filter delay time estimated as $0.506/f$, where f represents the filter cut-off frequency in Hz.

Fitting and Simulation

The data were fitted with various functions using the chi-squared method. Simulated macroscopic currents were numerically calculated using the Euler integration method. The integra-

tion step size was set by calculating, for each state, the sum of all the leaving rate constants and setting the step size to one half the reciprocal of the maximum sum.

RESULTS

A Large Amount of Charge Movement is Associated with the Activation Conformational Changes

Fig. 1 *A* shows the macroscopic current elicited by ShBΔ6-46 channels in response to 70 ms steps to voltages between −50 and +50 mV followed by a step to −65 mV. An estimate of the total amount of charge movement during the activation transitions can be made from a measurement of the voltage dependence of the steady-state probability of being open. This was estimated by two different methods. For the first method, the steady state probability of being open was calculated by the following

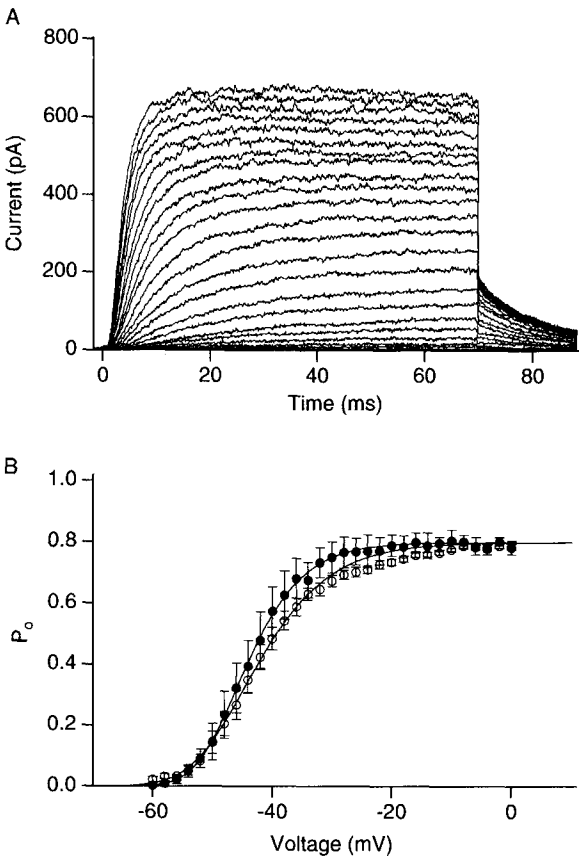

FIGURE 1. (*A*) Macroscopic currents from ShBΔ6-46. The currents were elicited in response to 70 ms pulses to voltages from −60 to 0 mV in increments of 5 mV followed by a step to −65 mV. The holding voltage was −100 mV. The data were filtered at 2 kHz and digitized every 89 μs. (*B*) Probability of being open, P_o, measured from the current during the pulse (*open circles*) and tail (*filled circles*). The P_o values measured from the pulse currents were calculated from the currents at the end of pulses >50 ms in duration divided by the driving force assuming a reversal voltage of −80 mV and normalizing to 0.8 at depolarized voltages. The P_o values measured from the tail currents were calculated from the current at −65 mV 500 μs following the pulses to the voltages indicated, and normalized to 0.8 at depolarized voltages. Error bars represent the standard error of the mean. The smooth curve through the pulse data points (*circles*) represents a fit of Eq. 3 with $n = 4$, $z = 3$ electronic charges and $V_{1/2} = -56$ mV. The smooth curve through the tail data points (*filled circles*) represents a fit of Eq. 3 with $n = 4$, $z = 4$ electronic charges and $V_{1/2} = -54$ mV. The curves were scaled to match the peak open channel probability determined from single-channel analysis ($P_o^{max} = 0.8$) (see Hoshi et al., 1994).

equation:

$$P_o = \frac{I}{iN} \tag{1}$$

where P_o is the probability of being open, I is the macroscopic current, i is the single-channel current, and N is the number of channels in the patch. The current, I, was measured between 50 and 150 ms after the initiation of the pulse, where activation had reached steady state at all of the voltages tested. The single-channel current (i) at each voltage was estimated from linear fits to the single-channel current-voltage relation measured between −30 and +30 mV. The number of channels (N) was estimated from Eq. 1 where I and i were measured at depolarized voltages, and P_o is the maximum P_o (P_o^{max}) determined from single-channel experiments. As shown in the previous paper (Hoshi et al., 1994), P_o^{max} is actually ~0.8 because of voltage independent transitions to nonconducting states after opening. Note, however, that the level of P_o^{max} does not significantly affect the estimates of charge movement in the following discussion. The second method of estimating the steady state P_o is from measurements of the instantaneous amplitude of the tail currents after each depolarizing voltage step. The tail currents were recorded after a 50 or 150 ms depolarizing pulse and were measured 0.5 ms after the initiation of the hyperpolarizing pulse. Because all of these measurements were made at −65 mV, the tail current amplitude is directly proportional to P_o at the end of the depolarizing pulse and was normalized to P_o^{max} at depolarized voltages as done for the first method.

The average steady-state probability of being open from a number of patches was calculated from the currents at the end of the pulse and at the beginning of the tail and is plotted as a function of voltage in Fig. 1 *B*. The P_o vs voltage relation from the tail currents has also been plotted on semilog axes in Fig. 2 *A*. The voltage-dependence of the equilibrium P_o for a simple two state system, where the equilibrium constant is exponentially dependent on voltage, is given by a Boltzmann distribution of the form:

$$P_o = \frac{1}{(1 + e^{-(V-V_{1/2})zF/RT})} \tag{2}$$

where V is membrane voltage, $V_{1/2}$ is the voltage at which half of the channels are activated, z is the equivalent charge movement, F is Faraday's constant, R is the universal gas constant, and T is the absolute temperature. The voltage-dependence of the equilibrium P_o for an activation mechanism involving n independent and identical conformational changes before opening would be described by the n^{th} power of Boltzmann distribution of the form:

$$P_o = P_o^{max}\left[\frac{1}{(1 + e^{-(V-V_{1/2})zF/RT})}\right]^n \tag{3}$$

where $V_{1/2}$ is the voltage where half of the independent and identical conformational changes have occurred, z is the equivalent charge movement for each conformational change, and n is the number of conformational changes. Fig. 2 *A* shows the fits of Eq.

3 with $n = 1$ (*dashed line*) and $n = 4$ (*solid line*). The steady state P_o vs voltage relation is poorly described by a Boltzmann distribution and is better described by a Boltzmann distribution raised to a power. This result is expected for a channel that must undergo a number of voltage-dependent transitions during activation.

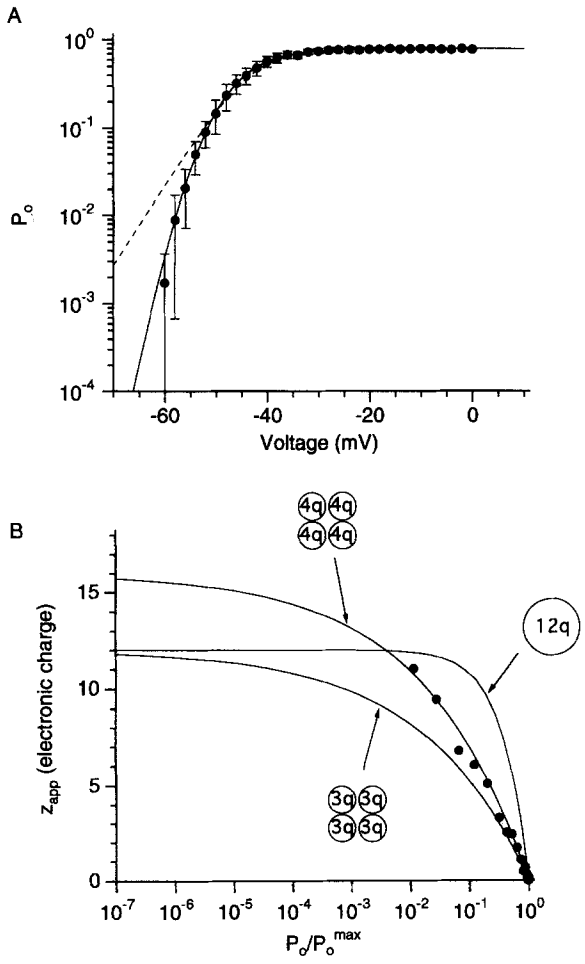

FIGURE 2. (*A*) A semi-logarithmic plot of the steady-state P_o vs voltage relationship obtained from the tail currents. The smooth line through the data points represents a fit of Eq. 3 with $n = 4$, $z = 4$ electronic charges and $V_{1/2} = -54$ mV. The dashed line represents a fit of Eq. 3 with $n = 1$, $z = 5.3$ electronic charges and $V_{1/2} = -43.1$ mV. (*B*) Apparent charge movement, z_{app}, estimated from the tail P_o vs voltage relationship at different P_o levels. The tail currents were elicited as in Fig. 1 and the derivatives dP_o/dV were measured using linear regression through three data points. The z_{app} was calculated using Eq. 4. The z_{app} at different P_o levels of three different models are also shown; a Boltzmann distribution with a total equivalent charge, z_{tot}, of 12 electronic charges (Eq. 3 with $n = 1$, $z = 12$ electronic charges), a fourth power of a Boltzmann distribution with $z_{tot} = 12$ electronic charges (Eq. 3 with $n = 4$, $z = 3$ electronic charges), and a fourth power of a Boltzmann distribution with $z_{tot} = 16$ electronic charges (Eq. 3 with $n = 4$, $z = 4$ electronic charges).

Because Boltzmann distributions with powers between 2 and 6 could produce very similar fits, the value of n was not well determined. However, since it is now clear that *Shaker* channels in *Xenopus* oocytes exist as a tetramer of four identical subunits (Liman, Tytgat, and Hess, 1992; MacKinnon, 1991), it is natural to consider the independent and identical conformational changes as a single conformational change

in each of four subunits, such as described by Hodgkin and Huxley (Hodgkin and Huxley, 1952) for voltage-dependent potassium channels in squid axons. The data were, therefore, fitted assuming $n = 4$ as expected if there were four independent and identical conformational changes during the activation process. The P_o vs voltage data calculated from the steady state current during the pulse were well fitted by Eq. 3 with $V_{1/2} = -56$ mV and $z = 3$ electronic charges (per subunit), whereas the P_o data from tail currents were better fitted with $V_{1/2} = -54$ mV and $z = 4$ electronic charges (per subunit) (Fig. 1 *B*). Despite this difference, both P_o vs voltage curves predict a large amount of charge movement associated with activation. Interpreting the fourth power of a Boltzmann distribution as above, these values of z indicate that the equivalent of 3 to 4 electronic charges move through the electric field across the membrane during the conformational change in each of the four subunits. This produces the equivalent of 12 to 16 electronic charges moving during the activation transitions in each channel.

The differences in P_o estimated from pulse versus tail current measurements could result from an error in estimating the P_o from the current during the pulse. To measure P_o from currents during the pulse, a linear approximation was made to estimate the single-channel current at low voltages. Because the single-channel current-voltage relation, $i(V)$, is somewhat outwardly rectifying at low voltages, this approximation may produce a systematic error in the open probabilities calculated from steady state current. The measurement of activation by tail current amplitudes does not require an estimate of the single-channel current and may represent a more reliable estimate of P_o.

Alternatively the differences in P_o estimated from pulse versus tail current measurements could result from a dependence of the early time course of the tail currents on the pulse voltage. This could result from one of two types of mechanisms: (*a*) a small voltage-dependence to the steady state P_o at depolarized voltages, or (*b*) potassium accumulation in an area near the outside surface of the membrane. As shown in the previous paper (Hoshi et al., 1994), the channel, once open, exhibits very weakly voltage-dependent sojourns in a relatively unstable closed conformation, *Cf*. A small voltage dependence to the equilibrium between the open state and *Cf* could produce a small increase in the P_o measured from the pulse currents at depolarized voltages. This small increase would not be present in the P_o measured from the tail currents because of a rapid equilibration (in 230 μs) between the open state and *Cf* during the tail currents. This effect, illustrated in the following paper, could account for much of the difference in the apparent steepness of the P_o vs voltage curves measured by the two methods.

The above estimate of the total amount of charge movement during the activation process is dependent on the exact form of the equation used to fit the steady state P_o vs voltage data. However, a less model-dependent method for estimating charge movement from the steady state P_o vs voltage data was suggested by Almers (1978), (see also Andersen and Koeppe, 1992). For any linear kinetic scheme for activation, the total amount of charge movement required for opening will be reflected in the limiting exponential rise in the voltage dependence of steady state P_o at very low P_o,

corresponding to the limiting slope of the steady state P_o vs voltage relation when plotted on semilog axes.

$$z_{tot} = \lim_{V \to -\infty} [z_{app}] \qquad \text{where} \qquad z_{app} = \left(\frac{RT}{F}\right) \frac{d[\ln (P_o)]}{dV} = \left(\frac{RT}{FP_o}\right) \frac{dP_o}{dV} \tag{4}$$

A test of having reached the true limiting slope is to plot the apparent charge movement z_{app} as a function of P_o. At negative voltages, this plot will asymptotically approach a saturating value equal to the total charge movement (z_{tot}). The apparent charge movement from the steady state P_o measured from tail currents is plotted as a function of P_o in Fig. 2 *B*. Because of the extremely small size of the current relative to the noise when the P_o was less than 10^{-3}, neither the steady state current during the pulse nor the amplitude of the tail currents could be recorded reliably in this range. Because the slope measurements were made over three data points the slope estimates of apparent charge movement could not be made when the P_o was much below 10^{-2}. While it appears from Fig. 2 *A* that the semilog plot of steady state P_o vs voltage has reached a limiting slope, the apparent amount of charge movement has not saturated when P_o is equal to 10^{-2}. The slope measurement at the lowest P_o that we could attain, corresponding to a total of ~10 electronic charges moving during activation, is clearly an underestimate of the charge movement.

The degree to which this estimate of charge movement might be an underestimate of the true charge movement was studied by examining the limiting slope estimates of apparent charge movement from different gating models. As will be shown in the following paper (Zagotta et al., 1994), for many models with multiple voltage-dependent conformational changes, the predicted voltage-dependence of P_o can be approximated by an n^{th} power of a Boltzmann distribution, where n is generally less than or equal to the number of voltage-dependent conformational changes. We have therefore considered three distributions for the voltage dependence of Po: (*a*) a Boltzmann distribution with $z = 12$ electronic charges; (*b*) a fourth power of a Boltzmann distribution with $z = 3$ electronic charges (making a total of 12 electronic charges); and (*c*) a fourth power of a Boltzmann distribution with $z = 4$ electronic charges (making a total of 16 electronic charges). The apparent charge movement from these models, calculated from Eq. 4, is plotted along with the data in Fig. 2 *A*. Notice that only the single Boltzmann distribution was sufficiently near its limiting slope by $P_o = 10^{-2}$ to produce an accurate estimate of the charge movement. Measurements from the fourth power of Boltzmann distributions underestimated the charge movement by 31% at $P_o = 10^{-2}$ and by 19% at $P_o = 10^{-3}$. Even if the amount of charge movement is changed, which has the effect of scaling these curves along the vertical axes, a single Boltzmann distribution could never produce an adequate fit to this transformation of the P_o data. Furthermore, a fourth power of a Boltzmann with $z = 4$ electronic charges per conformational change describes the data well. Therefore, whereas the limiting slope measurement of the data predicts only ~10 electronic charges moving during activation, the true charge movement could be as high as 16 electronic charges. This result is also supported by the voltage dependence of the gating charge (see Fig. 10 below). These values for charge movement are similar to those reported by Schoppa and co-workers (Schoppa, McCormack, Tanouye, and Sigworth, 1992), who estimated a charge movement of 9.5 electronic

charges from limiting slope measurements and 12.3 electronic charges from an analysis of gating currents.

Activation Is Likely to Require More than Five Conformational Changes

Whereas these steady-state measurements are limiting in what they reveal about the activation gating mechanism, a great deal more can be learned from an examination of the kinetics of the activation process. Fig. 3 *A* shows, on a rapid time scale, macroscopic currents from ShBΔ6-46 elicited by steps to voltages between −50 and +50 mV from a holding voltage of −100 mV. At each voltage, the currents can be seen to rise sigmoidally, reflecting the requirement for multiple conformational transitions before opening.

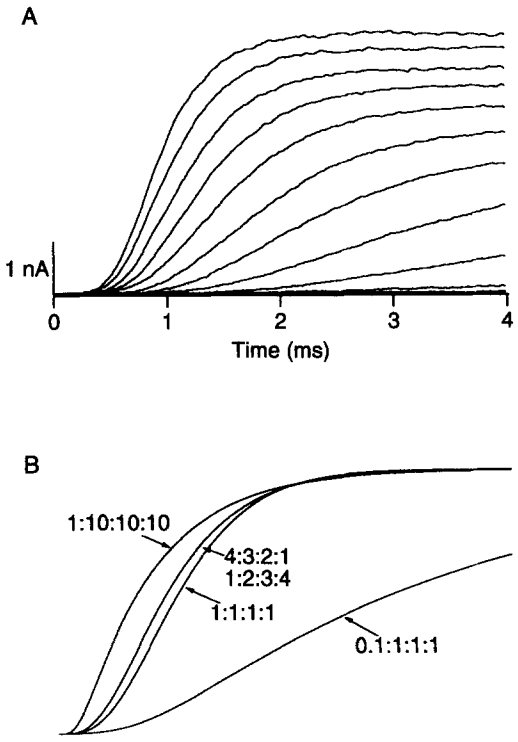

FIGURE 3. (*A*) Activation kinetics of macroscopic currents elicited in response to pulses from a holding voltage of −100 mV to voltages from −50 to +50 mV in increments of 10 mV. The data were filtered at 10 kHz and digitized every 12 μs. (*B*) Activation kinetics of ionic currents predicted by Scheme I with the indicated ratios of the four rate constants. The 4:3:2:1 and 1:2:3:4 schemes predict indistinguishable currents. The channels were set initially in the C_1 state.

The absolute amount of delay, however, is dependent on a number of factors including the number of conformational changes required to open the channel and the overall rate of the activation process. The most informative aspect of the delay, therefore, is not the absolute amount of delay, but the amount of delay relative to the overall rate of activation, which we will refer to as sigmoidicity. The relative sigmoidicity of different curves can be compared after scaling the time axis such that the time derivative at the half maximal values are equal. It depends on the number of conformational changes required to open the channel and their relative rate constants but not on the absolute value of the rate constant for any particular

conformational change. In general, an activation process involving four sequential conformational transitions may be summarized by the following gating scheme at depolarized voltages:

$$C_1 \xrightarrow{\alpha_1} C_2 \xrightarrow{\alpha_2} C_3 \xrightarrow{\alpha_3} C_4 \xrightarrow{\alpha_4} O$$

SCHEME I

where C_{1-4} represent closed conformations, O represents an open conformation and α_1 to α_4 represent the rate constants for the indicated conformational changes. At depolarized voltages, the rate constants for the reverse transitions would be expected to be much slower than the rates constants for the forward transitions (see below) and so are ignored here.

Fig. 3 *B* shows the calculated macroscopic activation for several different versions of Scheme I. An activation scheme involving four independent and identical conformational changes (such as Hodgkin and Huxley, 1952) would correspond to Scheme I where the relative values of α_1:α_2:α_3:α_4 are 4:3:2:1. However, if the conformational changes are not independent or not identical, the relative values may differ from 4:3:2:1. Previously, varying the relative values of the rate constants has been used as a way to model cooperative interactions between subunits in the channel (Gilly and Armstrong, 1982; Perozo, Papazian, Stefani, and Bezanilla, 1992; Vandenberg and Bezanilla, 1991). Fig. 3 *B* shows that relative rate constant values of 4:3:2:1 and 1:2:3:4 produce identical activation delays and sigmoidicity (Armstrong, 1981). This result underscores the difficulty in determining the rates of the activation transitions from measurements of macroscopic activation. The sigmoidicity is increased somewhat when the relative rate constant values are changed to 1:1:1:1. For this curve the rate constant value was adjusted so that the rate of rise at the half maximal current was similar to that of the 4:3:2:1 curves. However, if the delay is increased by the slowing of an early step in the activation process by a factor of 10, the primary effect is to slow down substantially the overall rate of activation, as shown by the curve labeled 0.1:1:1:1. After adjusting the rate constants to normalize the rate of rise at the half maximal current as before, it is clear that slowing down an early step has the effect of decreasing the amount of sigmoidicity (curve labeled 1:10:10:10). Furthermore, increasing a reverse rate constant has a similar effect to decreasing a forward rate constant. As can be seen in Fig. 4 *B*, the maximum sigmoidicity is generated when the relative rate constants for the forward transitions are 1:1:1:1. This sigmoidicity is only slightly greater than that produced by four independent and identical conformational changes (4:3:2:1). The only way of increasing the sigmoidicity beyond this maximum, while still maintaining time homogeneous rate constants, is to increase the number of transitions required to open the channel.

These constraints on the ways of producing sigmoidicity allow us to estimate the minimum number of conformational transitions required to open the ShBΔ6-46 channel. The predictions of the activation scheme shown below, involving four to eight independent and identical transitions, are compared to the macroscopic activation kinetics during steps to 0 and +50 mV in Fig. 4 *A*.

$$C_1 \xrightarrow{n\alpha} C_2 \xrightarrow{(n-1)\alpha} \cdots \xrightarrow{2\alpha} C_n \xrightarrow{\alpha} O$$

SCHEME II

where n represents the number of transitions. The rate constants for the reverse transitions were assumed to be zero at these depolarized voltages, and α was adjusted to fit the rate of rise at half maximal current. Comparison of the activation time

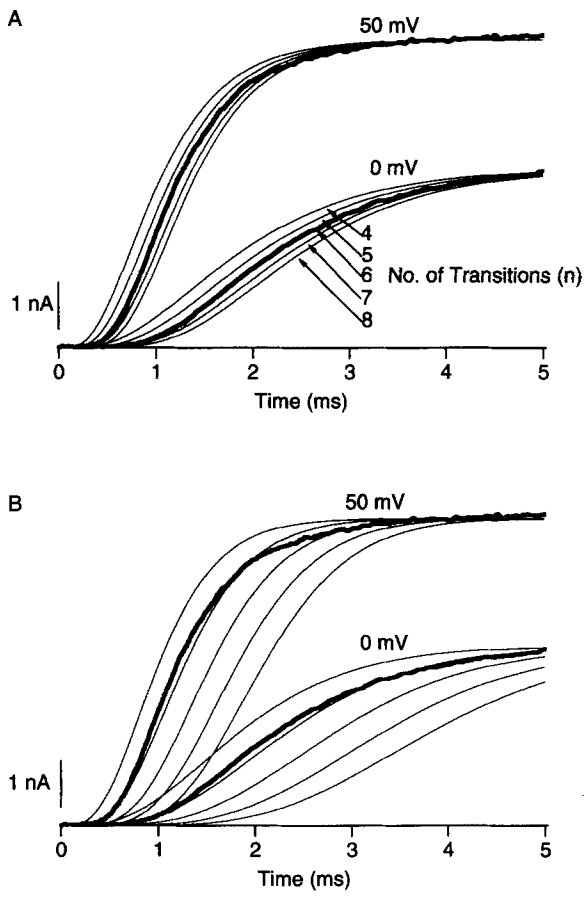

FIGURE 4. (*A*) Macroscopic currents elicited in response to pulses to +50 and 0 mV from a holding voltage of −100 mV (*thick lines*). Simulated currents from various independent models (Scheme II) with 4, 5, 6, 7, and 8 closed states (n) are shown superimposed. Backward rate constants are set to 0 and all of the channels are assumed to be in C_1 at $t = 0$. The forward rate constant α was adjusted so that the rate of rise at the half-maximum level was the same. The data are filtered at 10 kHz and digitized every 10 μs. (*B*) Simulated currents from cooperative models (Scheme III) with 4, 5, 6, 7, and 8 closed states (n) are shown superimposed on the measured currents at +50 mV and 0 mV (*thick lines*). All forward rate constants are set to α and the backward rate constants are set to 0. α was adjusted so that the rate of rise at the half-maximum level was the same. All of the channels are assumed to be in C_1 at $t = 0$.

courses of Scheme II with different values of n is shown in Fig. 4 *A*. This plot demonstrates that at least six independent and identical transitions are required to reproduce the observed sigmoidicity in the macroscopic activation.

As indicated above, if the independence constraint is relaxed, as in Scheme III, then more sigmoidicity can be generated.

$$C_1 \xrightarrow{\alpha} C_2 \xrightarrow{\alpha} \cdots \xrightarrow{\alpha} C_n \xrightarrow{\alpha} O$$

SCHEME III

If these five transitions arise from five identical, but not independent, conformational changes, then Scheme III can be viewed as a form of cooperativity, as discussed by Vandenberg and Bezanilla (Vandenberg and Bezanilla, 1991). As activation proceeds, the rate of the remaining conformational changes is increased so as to compensate exactly for the decrease in the number of remaining conformational changes. Fig. 4 *B* shows that in this special case, five transitions are sufficient to explain the sigmoidicity. However, this particular activation scheme, involving just five transitions, is inconsistent with the results shown below. Therefore, this analysis has suggested that a minimum of five to six transitions are required to open the channel.

This estimate of the number of transitions relies on a precise measurement of the sigmoidal time course that can be complicated by series resistance. However we believe that series resistance did not appreciably affect our measurements for the following reasons: (*a*) The capacity transient typically settled in <30 μs at high bandwidth. (*b*) The sigmoidal delay was nearly identical for patches with different size currents and for different size voltage steps between 0 mV and +100 mV (see Fig. 14). (*c*) The sigmoidal delay in the currents was also nearly identical to the sigmoidal delay seen in the cumulative distributions of first latencies (see Fig. 1 of the previous paper).

To estimate accurately the number of transitions in the activation pathway, we must insure that the channels are in states furthest from the open state at the beginning of the pulse. This can be tested by investigating the effect of holding voltage on the time course of macroscopic activation. Fig. 5 *A* shows the macroscopic currents elicited by voltage steps to 0 mV from holding voltages between −125 and −45 mV. The depolarized holding voltages caused a large decrease in the current amplitude due to steady state C-type inactivation (Hoshi et al., 1994). The activation time courses of the non-inactivated channels are compared in Fig. 5 *B* by normalizing the currents to their peak current amplitude. As originally shown by Cole and Moore (1960) for squid potassium channels, the depolarized holding voltages caused a decrease in the delay associated with the activation process. They interpreted this decrease in delay to mean that many of the channels at depolarized holding voltages resided in closed states along the activation pathway nearer to the open state. Upon depolarization, these channels were required to undergo fewer conformational transitions before opening and therefore exhibited less delay.

Cole and Moore (1960) further showed that if the currents were shifted along the time axis by an amount equal to the lost delay, the activation at different holding voltages followed exactly the same time course. This result suggests that the equilibrium distributions among the states at the different holding voltages represent intermediate distributions during the activation process from very hyperpolarized voltages. As shown by Cole and Moore (1960) and Hill and Chen (1971*a*,*b*), this property is found in any system described by the independent action of a number of first order transitions, such as the type of model proposed by Hodgkin and Huxley (1952). Fig. 5 *C* shows the results of this analysis on the activation of ShBΔ6-46

channels. The time course of the currents overlay nearly perfectly with holding voltages between −125 and −65 mV but is somewhat slower after holding voltages of −55 mV and −45 mV. This deviation from the Cole-Moore prediction only becomes ascertainable at holding voltages where there is an appreciable steady-state probability of being in the open state. This suggests that the activation of these potassium

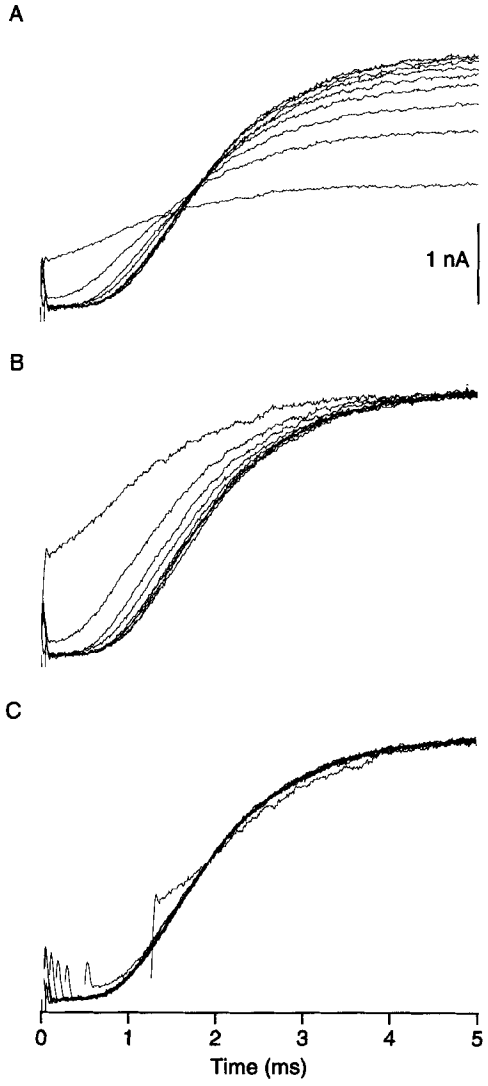

FIGURE 5. (*A*) Macroscopic currents recorded at 0 mV after 2 s prepulses to −40 to −140 mV in increments of −20 mV. The holding voltage was −90 mV. The data were filtered at 10 kHz and digitized every 10 μs. (*B*) The currents shown in *A* were scaled so that the current amplitudes were the same. (*C*) The scaled currents as shown in *B* were shifted along the time axis so that the half maximal points coincide.

channels deviates from the predictions of an independent gating scheme near the open state.

To determine a holding voltage at which the channels are no longer distributed among many closed states in the activation pathway but primarily populate a single resting closed conformation far from the open state, we examined the dependence of

the delay on the holding voltage (Perozo et al., 1992; Taylor and Bezanilla, 1983). Fig. 6 plots the time to half maximal current as a function of holding voltage between −125 and −45 mV from four different patches. The extent of the delay increases steadily with hyperpolarization and is nearly saturated at −100 mV. This result justifies the kinetic comparisons in Fig. 4 of the activation time course at holding voltages of −100 mV with the models. This saturation of the delay in ShBΔ6-46 channels occurs at a voltage considerably less hyperpolarized and with less delay than in squid potassium channels, which require 25 independent transitions to fit the delay in activation (Cole and Moore, 1960).

There Are Many Voltage-dependent Conformational Changes Associated with Activation

In the previous analysis we have argued that a considerable amount of charge movement is associated with the activation process (at least 12 to 16 electronic charges) and that activation involves many conformational transitions (at least 5 or 6).

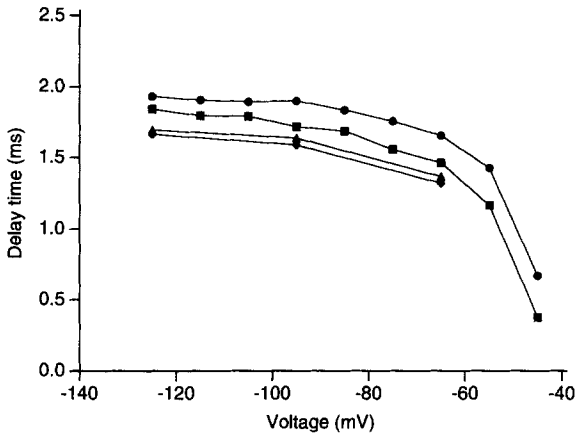

FIGURE 6. Effects of the prepulse voltage on the time to half maximal current recorded at 0 mV after 2 s prepulses to the voltages indicated. The macroscopic currents were elicited as in Fig. 5. Data from four different experiments are shown using different symbols.

In general, the activation process over the entire voltage range may be summarized by the following scheme:

$$C_1 \underset{\beta_1}{\overset{\alpha_1}{\rightleftarrows}} C_2 \underset{\beta_2}{\overset{\alpha_2}{\rightleftarrows}} \cdots \underset{\beta_{n-1}}{\overset{\alpha_{n-1}}{\rightleftarrows}} C_n \underset{\beta_n}{\overset{\alpha_n}{\rightleftarrows}} O$$

SCHEME IV

where α_1 to α_n represent the rate constants for the forward transitions and β_1 to β_n represent the rate constants for the reverse transitions and n is greater than or equal to 5. Because *Shaker* channels exist as a tetramer of *Shaker* subunits, this scheme precludes a process of activation involving only a single conformational change per subunit ($n = 4$). The total charge moved (at least 12 to 16 electronic charges) is the sum of the charge moved for each of the n transitions. Here we illustrate that the charge movement is probably spread out among many of the conformational transitions. The charge movement for each transition can be separated into two

components: the charge that moves between the occupied state and the transition state, and the charge that moves between the transition state and the destination state. The voltage dependence of the forward transitions (α's) is determined only by the charge moving before the transition state for a forward transition; similarly the voltage dependence of the reverse transitions (β's) is determined only by the charge moving after the transition state for a forward transition. Below we also demonstrate that for many of the conformational changes along the activation pathway, the voltage-dependence of the reverse transitions (β's) appears to be larger than the voltage-dependence of the forward transitions (α's) indicating that the charge movement is more prominent after the transition state for each forward conformational change.

Voltage dependence of the forward transitions. The voltage dependence of the forward transitions was examined by investigating the gating kinetics at voltages greater than −20 mV. At these depolarized voltages, the steady state P_o is nearly saturated (at P_o^{max}), and the rate constants for the reverse transitions are expected to be relatively small. This is a reasonable expectation because, in a multistep activation scheme, the steady state P_o will be near saturating only when the rate constants for the forward transitions are, on average, many times larger than the rate constants for the reverse transitions. Consider, for example, a scheme involving a number of independent and identical transitions summarized as follows:

$$C_1 \underset{\beta}{\overset{n\alpha}{\rightleftarrows}} C_2 \underset{2\beta}{\overset{(n-1)\alpha}{\rightleftarrows}} \cdots \underset{(n-1)\beta}{\overset{2\alpha}{\rightleftarrows}} C_n \underset{n\beta}{\overset{\alpha}{\rightleftarrows}} O$$

SCHEME V

where α represents the rate constant of the forward transition for the conformational change, β represents the rate constant of the reverse transition, and n is the number of transitions. For Scheme V the equilibrium constant for the elementary transition is given by the following equation:

$$K = \frac{\alpha}{\beta} = \frac{P_o^{1/n}}{1 - P_o^{1/n}} \tag{5}$$

Therefore, an activation process involving a single conformational change ($n = 1$) will have a steady-state open probability of 0.95 relative to P_o^{max} only when the rate constant of the forward transition is 19 times greater than the rate constant of the reverse transition. Furthermore, an activation process involving eight independent and identical conformational changes ($n = 8$) will have a steady state open probability of 0.95 relative to P_o^{max} only when the rate constant of the forward transition for each conformational change is 155 times larger than the rate constant of the reverse transition. The addition of a voltage-independent closed state not in the activation pathway, as suggested in the previous paper (Hoshi et al., 1994), will decrease P_o^{max} below one and cause a small increase in the rate of the reverse transitions relative to the forward transition for a given P_o/P_o^{max}.

To estimate the voltage dependence of the forward transitions during activation we have examined the voltage dependence of several parameters measured from the activation time course at depolarized voltages. First, the rate of activation was

estimated by fitting a single-exponential function to the latter phase of the activation process, beginning at the time of the half maximal current, as shown in Fig. 7 *A*. For an activation process involving multiple independent and identical conformational changes, like that described by Scheme V, the time course of activation from the C_1 state is given by the following equation:

$$P_o = \left[\left(\frac{\alpha}{\alpha + \beta}\right)(1 - e^{-(\alpha+\beta)t})\right]^n \tag{6}$$

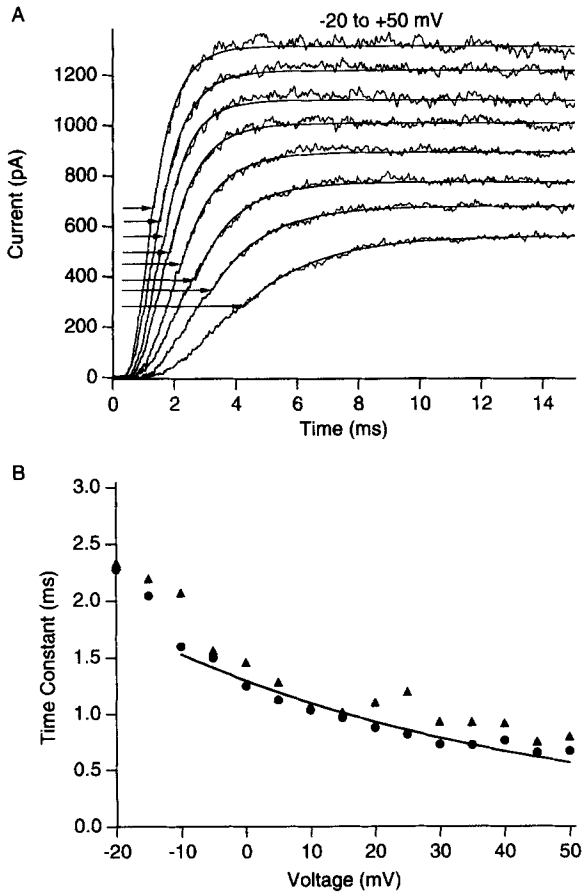

FIGURE 7. The rate of activation as estimated by a single exponential fit to the late phase of activation. (*A*) The macroscopic currents recorded with voltage pulses to −20 to 50 mV in increments of 10 mV are shown. The data are fitted with single exponentials beginning at the half maximal times indicated by the arrows. The data were filtered at 10 kHz and digitized at 20 μs. The holding voltage was −100 mV. (*B*) Time constants of the late phase of activation as measured in *A* are plotted against the voltage. The different symbols are from two separate experiments. The line represents an exponential function with an equivalent charge of 0.42 electronic charges.

In general, the relaxations of any system of s states will be multiexponential with $s - 1$ characteristic time constants (Hille, 1992). The macroscopic activation time course of Scheme V, with $n + 1$ states, will contain n characteristic time constants given by the following equations:

$$\tau_1 = \frac{1}{(\alpha+\beta)}, \tau_2 = \frac{1}{2(\alpha + \beta)}, \cdots \tau_n = \frac{1}{n(\alpha + \beta)} \tag{7}$$

The slowest time constant, τ_1, will dominate the activation time course at long times. In addition, at depolarized voltages (> -20 mV) $\alpha \gg \beta$, so $\tau_1 = 1/\alpha$. Below -20 mV, the rate of the reverse transitions (β) will have a noticeable effect on the time constants. Therefore, for a scheme involving multiple independent and identical conformational changes, the time constant of the final phase of activation would be approximately equal to the reciprocal of the rate constant of each forward conformational transition, α, at depolarized voltages. As shown in Fig. 7 *B*, a single-exponential curve fitted to the voltage dependence of this time constant above -20 mV indicates that the rate of the forward transitions increases e-fold per 61 mV. This corresponds to the equivalent of 0.42 electronic charges moving through the membrane field between the resting state and the transition state for the slowest of the conformational changes in the activation pathway. It will be shown later that approximately this amount of charge movement must be associated with virtually all of the activation transitions.

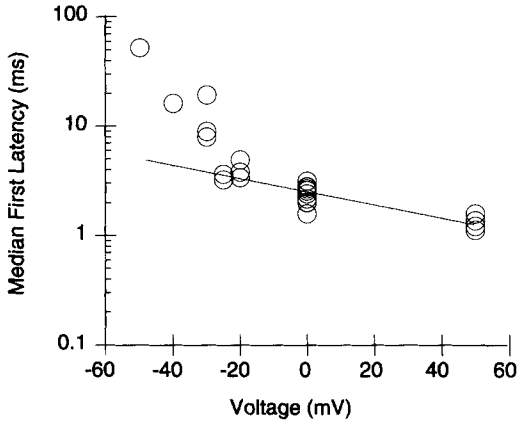

FIGURE 8. Voltage dependence of the median first latency. Median first latencies were measured from a number of single ShBΔ6-46 channels from different experiments as described in the proceeding paper (Hoshi et al., 1994). The straight line represents a single exponential function with an equivalent charge of 0.34 electronic charges.

The activation time course is best measured by the distribution of the latencies to first opening. As shown in the previous paper, the time course of the first latency distribution almost completely determines the time course of macroscopic activation at depolarized voltages. Fig. 8 shows the voltage dependence of the median first latency. The single-exponential curve shown fitted to these data above -20 mV indicates that the median first latency increases e-fold per 75 mV. This voltage dependence is very similar to that determined from the exponential fits to macroscopic activation and corresponds to an equivalent charge movement of 0.34 electronic charges.

The rate constants for the forward transitions near the open state, such as α_n and α_{n-1} in Scheme IV, can be estimated by examining the reactivation of the channels as shown in Fig. 9 *A*. Reactivation is measured using a pulse paradigm whereby the channels are first moved to the open state by a pulse to a depolarized voltage. Then, a small fraction of the channels ($< 20\%$) are allowed to close by a brief hyperpolarizing pulse, and these channels are reactivated by a second depolarizing pulse. As shown in Fig. 9 *B*, the time course of this reactivation is well described by a single

exponential function indicating that most of the channels that have closed can reactivate by undergoing just one or a small number of transitions. Therefore this method, previously used on other voltage-dependent channels (Gilly and Armstrong, 1982; Oxford, 1981; White and Bezanilla, 1985), allows an approximate measurement of the rate of the forward transitions near the open state. Also as shown in Fig. 9 *A*, by varying the voltage of the second depolarizing pulse we can estimate the

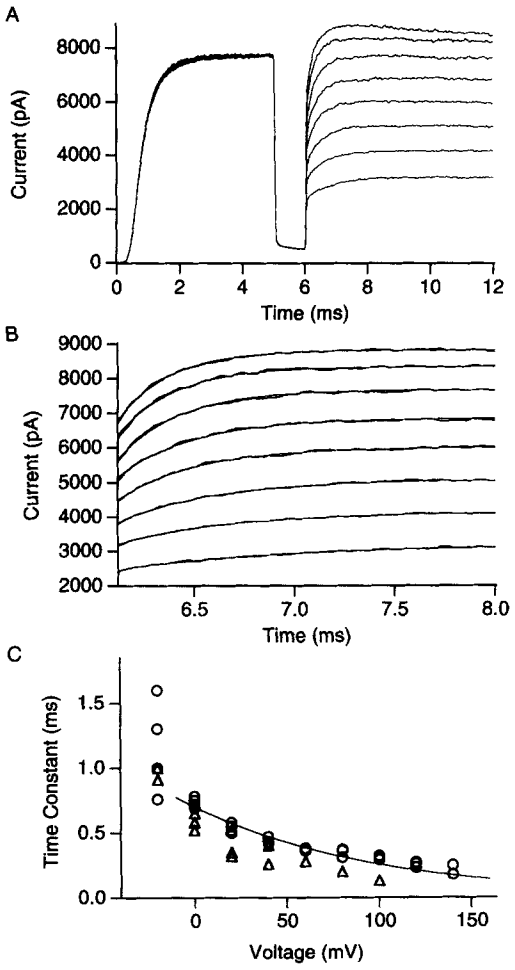

FIGURE 9. Estimation of the rate of the forward transitions using a double-pulse reactivation protocol. (*A*) The patch was depolarized by the first pulse to +50 mV for 10 ms, repolarized to −65 mV for 1 ms, and then depolarized by the second pulse to −20 to +140 mV in increments of 20 mV. The data were filtered at 10 kHz and digitized every 16 μs. The internal solution did not contain any added $MgCl_2$ because of block of the channels by Mg^{++} at high voltages. (*B*) The current recorded in response to the second pulse in the paradigm shown in *A* on a faster time scale. Single exponential fits are shown superimposed. (*C*) Voltage dependence of the time constant of reactivation. The time constants of the exponential fits to the current elicited by the second pulse are shown. Different symbols represent different experiments. The smooth curve represents a single exponential function with an equivalent charge of 0.26 electronic charges. These data were obtained from patches with somewhat faster kinetics than the patches used in Fig. 7. See Zagotta et al. (1994) for a discussion of variability between patches.

voltage dependence of these forward transitions. In Fig. 9 *C*, the time constant of reactivation is plotted as a function of voltage and is fitted with a single-exponential function with a voltage dependence of e-fold per 100 mV corresponding to 0.26 electronic charges. Note that this estimate of the charge movement associated with the forward transitions near the open state is very similar to the estimate of the

charge movement from the entire activation transitions from the previous two types of measurements.

The time constant of reactivation at any given voltage is similar to the time constant of the final phase of activation, shown in Fig. 7 *B*. The similarity in the time course of reactivation to that of the later phase of activation is also shown later in Fig. 15 where the time courses of reactivation and activation are overlaid. This similarity has a direct bearing on the activation gating schemes discussed in Figs. 3 *B* and 4 *B* involving nonindependent transitions. The schemes involving any number of independent and identical transitions, summarized by schemes II and V, predict that the time courses of reactivation and later phase of activation would be identical, with a time constant of $1/\alpha$. However the nonindependent kinetic schemes where all of the forward rate constants are equal, such as Scheme III, would predict that the reactivation time course would be almost two times faster than the later phase of activation, and Scheme I with relative rate constant values 1:2:3:4 predicts that reactivation would be almost four times faster. The reactivation results are consistent with all of the forward transitions behaving as a series of identical and independent conformational changes and exhibiting relatively little voltage dependence (~ 0.4 electronic charges each) compared to the overall charge movement associated with activation (12 to 16 electronic charges).

The rate constants for the forward transitions distant from the open state, such as α_1 and α_{n-1} in Scheme IV, can be studied by examining the time course of the ON gating currents during depolarizing voltage steps, as shown in Fig. 10 *A*. These gating currents were recorded in membrane patches containing many channels ($> 10{,}000$) where the ionic current through the channels was eliminated by ion substitution and the linear capacitance was subtracted, as described in the methods. The currents arise from the intrinsic charge movements occurring during the many voltage-dependent transitions of the activation pathway, and their time course is determined by the rate of occurrence and the charge movement of the gating transitions. As shown in Fig. 10 *A*, these ON gating currents did not follow a single exponential decay time course, as expected for a simple first order transition. Instead, at the depolarized voltages, they consistently exhibited a small rising phase followed by a roughly single-exponential relaxation. The small spike of current immediately after the voltage step was not always observed and is probably an artifact of the transient cancellation. A small rising phase in the ON gating current has also been seen in other voltage-dependent potassium channels (Bezanilla, Perozo, Papazian, and Stefani, 1991; Perozo et al., 1992; Taglialatela, Kirsch, VanDongen, Drewe, Hartmann, Joho, Stefani, and Brown, 1992; Taglialatela, Toro, and Stefani, 1992; White and Bezanilla, 1985). It is often interpreted to indicate nonindependent gating during the activation transitions. However, it has also been shown, in some cases, to arise as an artifact in the protocol to subtract the linear capacitance (Stuhmer et al., 1991). The rising phase shown in Fig. 10 *A* was seen with several different subtraction protocols, suggesting that it is a genuine property of the ON gating current. It is analyzed in more detail in terms of specific models for activation in the following paper. To measure the voltage dependence of the forward transitions, the time course of the relaxation of the ON gating currents was examined by fitting the decaying phase with a single exponential function. The voltage dependence of the

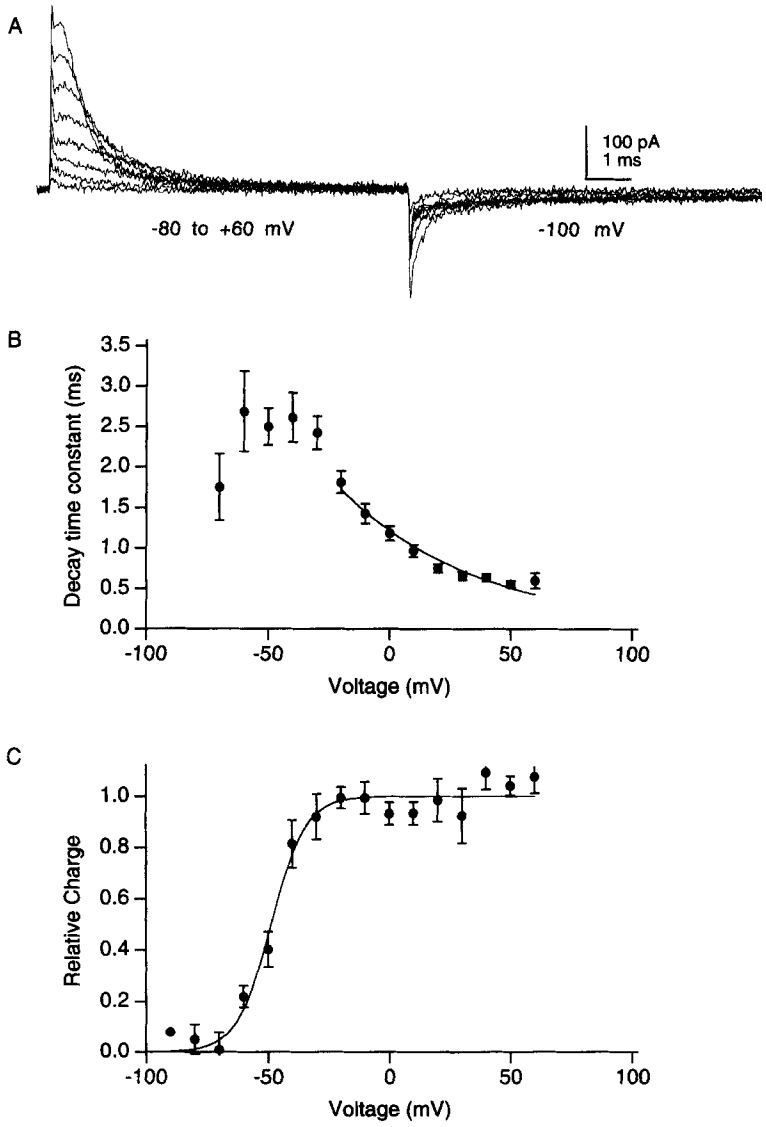

FIGURE 10. (*A*) The gating currents were elicited in response to 8-ms voltage pulses to −80 to +60 mV in increments of 20 mV from a holding voltage of −100 mV. The data were filtered at 8 kHz and digitized every 16 μs. (*B*) Time constants of the ON gating current decay are plotted against the voltage. The declining phases of the gating currents were fitted with single exponentials. A single exponential fit to the voltage dependence data (−20 to +60 mV, *smooth line*) shows an equivalent charge of 0.45 electronic charges. (*C*) Voltage dependence of the charge movement. The ON gating currents in response to 16-ms pulses were integrated and the normalized charge is plotted against the test voltage. Any residual current at the end of the 16-ms pulse was subtracted. The smooth curve is a Boltzmann fit to the data with an equivalent charge of 3.6 electronic charges and a half maximal voltage of −48.6 mV. The data were obtained from 19 different experiments. The error bars represent the standard error of the mean.

relaxation time constant is plotted in Fig. 10 *B*. The single-exponential curve shown fitted to these data > -20 mV indicates that the forward transition that determines the time course of the ON gating currents involves the movement of 0.45 electronic charges for the transition state, very similar to the previous estimates 0.34 to 0.42 charges made from the ionic currents.

ON gating currents similar to the ones shown in Fig. 10 *A* were integrated during 16 ms pulses to various voltages to estimate the net amount of charge movement occurring during the activation process at different voltages. This charge movement was normalized to the maximum charge movement at depolarized voltages, averaged from a number of patches, and is plotted as a function of voltage in Fig. 10 *C*. A scheme involving multiple independent and identical transitions, such as Scheme V, with rate constants that depend exponentially on voltage, predicts that the voltage dependence of the net charge movement will be described by a Boltzmann distribution. The slope of the distribution is directly related to the charge movement associated with each elementary transition. The fits of a Boltzmann distribution to the data in Fig. 10 *C* suggest that the charge movement for each elementary transition is equivalent to ~ 3.59 electronic charges. This is approximately one fourth of the total charge estimated from the P_o vs voltage curves in Figs. 1 and 2, but is significantly more than the 0.4 electronic charges associated with each forward transition.

All of the kinetic parameters for measuring the rates of the forward transitions at depolarized voltages—the rate of the final phase of activation, the median first latency, the rate of reactivation, and the rate of relaxation of the ON gating currents—exhibited a similar degree of voltage dependence. This voltage dependence corresponds to an equivalent charge movement of 0.3 to 0.5 electronic charges between the resting state and the transition state. Approximately this amount of charge movement must be associated with many of the forward transitions in the activation pathway. If only a few rate limiting transitions had this degree of voltage dependence the time course of activation at depolarized voltages would become significantly less sigmoidal. As will be shown later, the sigmoidicity is unchanged between 0 and +100 mV. An equivalent charge movement of 0.3 to 0.5 electronic charges, even if it is occurring for each of six or eight transitions, still represents a small fraction of the total charge movement estimated for the activation process from the steady state P_o vs voltage relations (12 to 16 electronic charges). Therefore, it is likely that a large portion of the charge is moving after the transition state for the conformational change and is therefore not apparent in the voltage dependence of the forward transition. We cannot rule out the possibility that the activation process contains, in addition, a small number of rapid, highly voltage dependent transitions. However, such a transition could not be the first transition in the activation pathway because it would produce an initial, rapid decay in the ON gating currents, instead of the small rising phase or plateau that is observed. In addition it could not be the last transition before opening where it would produce highly voltage dependent closed times and reactivation kinetics. Furthermore, if these rapid, highly voltage dependent forward transitions occurred, they would become exceedingly fast at depolarized voltages and would therefore not contribute significantly to the delay discussed above. We conclude, therefore, that many, and perhaps all, of the forward transitions in the activation pathway exhibit a similar degree of voltage dependence, corre-

sponding to the movement of 0.3 to 0.5 electronic charges between the resting state and the transition state.

Voltage dependence of the reverse transitions. If only a small portion of the charge movement is occurring between the resting state and the transition state for the activation transitions, then a large portion of the charge must be moving after the transition state. The charge movement occurring after the transition state should be apparent in the voltage dependence of the reverse transitions. Just as the rate of the

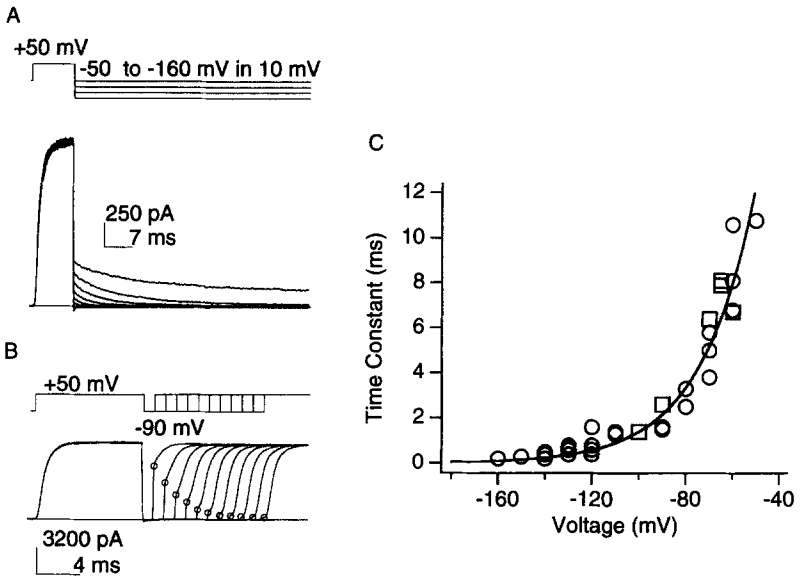

FIGURE 11. (*A*) Estimation of the deactivation kinetics by the tail current. The tail currents were measured at various voltages between −50 and −160 mV after 10-ms pulses to +50 mV and were fitted with single exponentials. The data were filtered at 3 kHz and digitized every 34 μs. (*B*) Estimation of the deactivation kinetics by the two-pulse protocol. The patch was depolarized to +50 mV for 10 ms, repolarized to a test voltage (−90 mV shown) for various durations, and repolarized to +50 mV. The envelope of the instantaneous current amplitudes at the beginning of the second depolarizing pulse (*circles*) shows the deactivation time course at this test voltage. This deactivation time course was fitted with a single exponential. The data were filtered at 4 kHz and digitized every 20 μs. (*C*) Voltage dependence of the deactivation time constant measured by the tail current method (*circles*) and by the two-pulse method (*squares*). The data were fitted with a single exponential with an equivalent charge of 1.1 electronic charges.

forward transitions was estimated by measuring the opening rate of the channels, or activation, at depolarized voltages, the rate of the reverse transitions was estimated by measuring the closing rate of the channel, or deactivation, at hyperpolarized voltages. Tail currents were recorded at hyperpolarized voltages following pulses to depolarized voltages (Fig. 11 *A*). The time courses of the tail currents become more rapid as the voltage is made more negative and are reasonably well fitted by single exponential functions, especially below −80 mV. The deactivation time course was

also estimated using a two pulse protocol (Fig. 11 *B*), where the extent of deactivation was measured as the instantaneous current at the beginning of the second pulse after allowing deactivation to occur for variable amounts of time between pulses. This two pulse protocol, while providing a lower resolution measurement of the deactivation time course, is much less sensitive to extracellular potassium accumulation during the first pulse (Swenson and Armstrong, 1981).

The apparent time constant of deactivation from a number of patches is plotted as a function of voltage in Fig. 11 *C*. Both the direct measurements of tail currents (*circles*) and the two pulse measurements (*squares*) produced similar estimates of deactivation time constants indicating that there was no noticeable problem with potassium accumulation affecting the time course of the tail currents in these experiments. The voltage dependence of the rate of the reverse transitions was estimated by fitting a single exponential function to the voltage dependence of the deactivation time constant (Fig. 11 *C*). This exponential function changes e-fold per 24 mV suggesting an equivalent gating charge movement of 1.1 electronic charges for the reverse transitions, two to three times larger than the charge movement seen in the forward transitions. Note that, as for the time constants of the activation transitions, the time course of deactivation may reflect many conformational transitions, including the forward transitions, and is therefore not a reliable estimate of the absolute rate constant or voltage dependence of any particular closing transition.

The analysis of single-channel data provides a more direct measurement of the rate and voltage dependence of transitions near the open state. In the previous paper we showed that the open durations were voltage-dependent at hyperpolarized voltages indicating that the channel can undergo a voltage-dependent closing transition to the activation pathway. Furthermore the voltage-dependence of the open durations and total open time during a burst indicated that the rate of this closing transition decreased e-fold per 22 mV of depolarization, corresponding to an equivalent gating charge movement of 1.1 electronic charge moving through the field between the open state and the transition state to closing. Note that this estimate of charge movement for the first closing transition is nearly identical to the estimate from the voltage dependence of macroscopic deactivation.

For a number of voltage-dependent potassium channels, it has been shown that various external monovalent cations can alter the rate, and occasionally the voltage-dependence of the deactivation process (Cahalan, Chandy, DeCoursey, and Gupta, 1985; Matteson and Swenson, 1986; Sala and Matteson, 1991; Shapiro and DeCoursey, 1991*a;* Shapiro and DeCoursey, 1991*b;* Spruce, Standen, and Stanfield, 1989; Swenson and Armstrong, 1981). To estimate the effect that external cations might have on the rate and voltage-dependence of the closing transitions, we have measured the macroscopic deactivation time course with different concentrations of external potassium and rubidium. Fig. 12 *A* shows the tail currents in 140 mM external potassium (*top*) and rubidium (*bottom*), recorded during repolarizations to voltages between −40 and −140 mV after depolarizing pulses. The tail currents were fitted with single-exponential functions, shown superimposed on the traces in Fig. 12 *A*. In general, the time courses of these tail currents were better described by a double-exponential than by a single-exponential function. This is particularly evident with voltage steps to −120 and −140 mV in both potassium and rubidium, in which

the tail currents contain a slow component that departs from the single-exponential time course. This multiple exponential character indicates that these tail currents involve more that just one open and one closed state, as more directly shown in the previous paper from an analysis of the single-channel currents during deactivation in 140 mM external potassium. In fact, the double-exponential tail currents are quite well described by Scheme VIII of the previous paper involving two closed states, *Cf* and *Ci* not in the activation pathway.

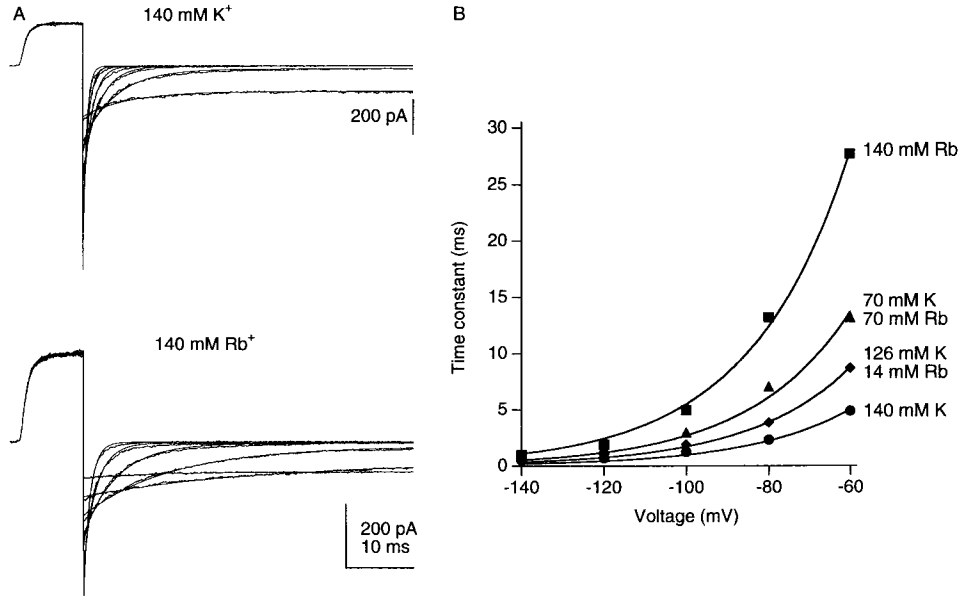

FIGURE 12. (*A*) Tail currents recorded in the outside-out configuration in the presence of 140 mM KCl (*top*) and 140 mM RbCl (*bottom*) in the extracellular solution. The currents were elicited in response to 10 ms voltages pulses to +50 mV followed by pulses to −40 to −140 mV in 20-mV increments. Single exponential fits to the tail currents are also shown superimposed (*smooth curves*). The data were filtered at 5 kHz and digitized every 59 μs. (*B*) Voltage dependence of the time constants in the tail currents recorded in the presence of external 140 mM K^+ (*circles*), 126 mM K^+ and 14 mM Rb^+ (*diamonds*), 70 mM K^+ and 70 mM Rb^+ (*triangles*), and 140 mM Rb^+ (*squares*). The external solution contained (in millimolar): 140 KCl and/or RbCl, 6 $MgCl_2$, 5 HEPES, pH 7.1 (NaOH). The concentration of KCl and RbCl together was 140 mM. The tail currents were fitted with single exponentials and their time constants are plotted. The smooth lines represent exponential fits to the voltage dependence of the time constants with an equivalent charge of one electronic charge.

Despite the multiple-exponential character of the tail currents, single-exponential fits provide an estimate of the rate and voltage-dependence of the closing transition to the activation pathway. Fig. 12 *B* plots the time constant of these exponential fits as a function of voltage for different concentrations of external potassium and rubidium. The voltage dependence of the time constant below −60 mV was estimated from a single-exponential fit shown superimposed on the data. For each of the solutions the time constant increased e-fold per 24 mV, nearly identical to the voltage

dependence of the deactivation time constant in normal solutions (e-fold per 24 mV) and the voltage dependence of the rate for closing to the activation pathway calculated from single-channel data (e-fold per 22 mV), as shown in the previous paper (Hoshi et al., 1994). Furthermore, in 140 mM external potassium (*filled circles*) the absolute time constant at −100 mV (1.2 ms) is very similar to the time constant in normal solutions (1.3 ms). Taken together, these results indicate that deactivation in 140 mM external potassium is not markedly different from deactivation in normal solutions, and that the parameters estimated from a single exponential fit provide a reasonable estimate of the voltage dependence of the closing transition.

In contrast to external potassium, external rubidium has a marked effect on the deactivation time course. This has been proposed to occur by a mechanism in which the channel cannot close when the pore contains an ion, referred to as the occupancy hypothesis (Ascher, Marty, and Neild, 1978; Marchais and Marty, 1979; Matteson and Swenson, 1986; Swenson and Armstrong, 1981). Rubidium, which has been reported to exhibit a longer residency within the pore of some potassium channels (Matteson and Swenson, 1986; Sala and Matteson, 1991), would therefore decrease the apparent closing rate. The similarity in the voltage dependence of the deactivation time constants in potassium and rubidium suggests that voltage dependence to the occupancy of these ions does not contribute markedly to the estimate of 1.1 electronic charges for the charge movement of the closing transition.

Note that these estimates of the amount of charge movement for a reverse transition in the activation pathway are two to three times larger than the charge movement estimated for the forward transitions. This suggests, as already indicated, that most of the charge movement for the activation transitions occurs after the transition state. The total charge movement for each transition would be the sum of the charge movement before the transition state and the charge movement after the transition state, or ~1.6 electronic charges. The channel would have to undergo 8 to 10 such transition to produce the 12 to 16 electronic charges estimated for the total charge movement of the activation process from the steady state P_o vs voltage relations. This agrees reasonably well with the estimated minimum of six independent and identical transitions required to account for the sigmoidicity in the activation time course. However, the movement of 1.6 electronic charges per transition does not agree well with the estimate of 3.59 electronic charges per transition from the voltage dependence of the net charge movement. This difference could result from cooperative interactions between subunits and/or multiple transitions per subunit.

The First Closing Transition Is Slower than Expected for Independent Transitions

In the proceeding discussion, the rate and voltage dependence of the reverse transitions were estimated from an analysis of the deactivation of macroscopic and single-channel currents. The time course of channel deactivation at hyperpolarized voltages will be dominated by the rates of the reverse transitions near the open state, such as β_n and β_{n-1} in Scheme IV. The possibility, therefore, exists that the reverse transitions more distant from the open state have very different rates and/or voltage dependences. To explore this possibility, we have investigated how the rate of the reverse transitions near the open state might be related to the rate of the reverse

transitions more distant from the open state. Scheme V, with independent and identical transitions, predicts that all of the forward rates will have the same voltage dependence, and all of the reverse rates will have the same voltage dependence. Furthermore, it predicts that the relative values of the rate constants for the forward transition will be n:(n − 1):. . . :2:1, as indicated earlier for Scheme II, and the relative values of the rate constants for the reverse transitions will be 1:2:. . . :(n − 1): n. The extent to which the channel behavior deviates from these predictions has a direct bearing on the physical mechanism underlying the activation process.

A fit of Scheme V (independent and identical transitions) to the steady state properties in Figs. 1 and 2 predicts a much faster time course of deactivation than is actually observed. This can be illustrated for the steady state and kinetic data at −60 mV. Fig. 2 *A* shows that the steady state probability of being open at −60 mV is ~0.001. From Eq. 5 with eight independent and identical transitions at −60 mV, this corresponds to an equilibrium constant at −60 mV, K_{-60}, of 0.73. In Fig. 7 we estimated α at depolarized voltages from exponential functions fit to the final phase of activation. These measurements indicated that α has a value of about 1,000 s^{-1} at 0 mV and increases e-fold per 60 mV. Extrapolation of this estimate of α down to −60 mV gives α_{-60} = 368 s^{-1}. Substituting K_{-60} and α_{-60} into Eq. 4 gives β_{-60} = 504 s^{-1}. The deactivation time course predicted for Scheme V will, in general, be multiexponential with time constants given by the expressions in Eq. 7. For eight independent and identical transitions at −60 mV, the predicted time constants would range from 0.14 ms to 1.1 ms. These time constants are much faster than the observed deactivation time constant at −60 mV (7 ms, Fig. 11). In particular, the dominant time constant predicted for deactivation, 0.14 ms, is over 50 times faster than the observed deactivation time constant. Similarly any activation mechanism involving 2 to 16 independent and identical conformational changes predicts a deactivation time course considerably faster than is actually observed.

This slow apparent closing transition manifests itself on other aspects of the kinetic behavior of the channel. One of these effects is on the sigmoidicity of the activation time course at hyperpolarized voltages. As described earlier, the sigmoidicity is defined as the amount of delay relative to the overall rate of activation and reflects the requirement for the channel to undergo many conformational changes before opening. The sigmoidicity in the activation time course at different voltages can be compared by first scaling the currents to the same steady-state level, and then adjusting their time scales to make the rate of rise at the half maximal current similar, as done in Fig. 3 *B*. Fig. 13 shows the macroscopic currents elicited by voltage steps to −50, −40, 0, and +50 mV before (*A*) and after (*B*) this normalization procedure. The normalization reveals the rather unexpected finding that the activation time courses at −40 and −50 mV exhibit substantially less sigmoidal character than the activation at 0 and +50 mV. In fact the activation of the currents at −40 and −50 mV is nearly a single exponential process. This is a direct contradiction of the predictions of an activation process involving multiple independent conformational changes, such as Scheme V. Fig. 13 *C* shows the predictions of Scheme V for eight independent and identical transitions using the rate constants and voltage dependencies determined above. While qualitatively these predictions appear to describe the data shown in Fig. 13 *A*, after normalization, shown in Fig.

13 *D*, it is clear that the sigmoidicity is the same at these voltages. In fact, all models with any number of independent first order transitions will produce the identical sigmoidal character at different voltages. This is evident in Eq. 6 for the time course of the open probability for n independent and identical transitions. For a given number of transitions n, the time course of the normalized currents depends only on the value of $(\alpha + \beta)t$. Therefore, by adjusting the time scale, the normalized currents at different voltages can exactly coincide.

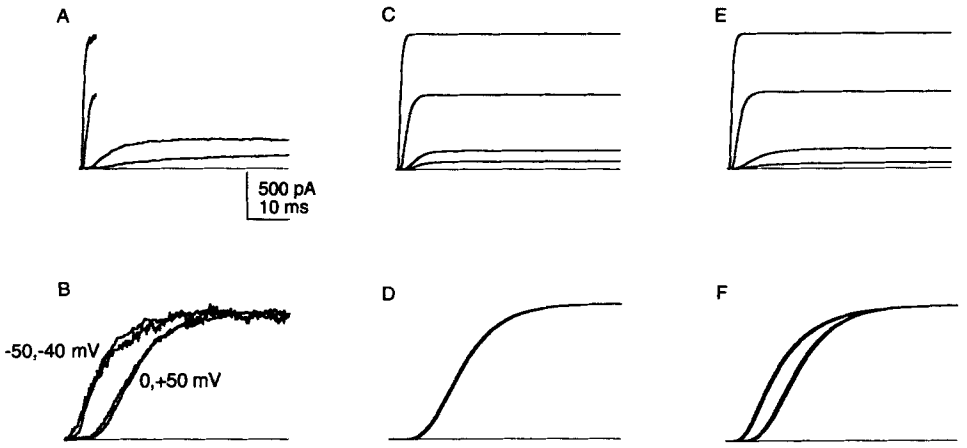

FIGURE 13. Sigmoidicity of the ionic currents recorded at −50, −40, 0, and +50 mV from the holding voltage of −100 mV. (*A*) Unscaled ionic currents at −50, −40, 0, and +50 mV. The +50 and 0 mV data were filtered at 10 kHz and digitized every 12 μs. Those at −40 and −50 mV data were filtered at 1 kHz and digitized at every 417 μs. (*B*) The currents shown in *A* after the normalization to compare the sigmoidicity. The currents are scaled vertically and horizontally so that their peak amplitudes and the slopes at the half-maximal amplitudes are the same. (*C*) Macroscopic currents simulated at −50, −40, 0, and +50 mV with Scheme V using eight independent and identical transitions (see text). The forward and backward rate constant values were determined as described in the text. All the channels were set to be in state C_1 at time zero. A linear $i(V)$ with the reversal voltage of −75 mV was assumed. (*D*) The simulated macroscopic currents shown in *C* were scaled as in *B* to compare the sigmoidicity. The sweeps for −50, −40, 0, and +50 mV essentially superimpose. (*E*) Macroscopic currents at −50, −40, 0, and +50 mV simulated using Scheme VI (see text) with $n = 8$ and $\theta = 10$ (see text). All the channels were set to be in state C_1 at time zero. A linear $i(V)$ with the reversal voltage of −75 mV was assumed. (*F*) The simulated macroscopic currents shown in *E* were scaled as in *B* to compare the sigmoidicity. The two left most sweeps are for −50 and −40 mV and the remaining two sweeps are for 0 and +50 mV.

The decreased sigmoidicity at hyperpolarized voltages could come about from at least two classes of mechanisms. (*a*) At hyperpolarized voltages, a single or small number of conformational changes could become rate limiting for the activation process because of a slow rate constant. This mechanism would require that the rate constant of one conformational change has a much greater voltage dependence than the other rate constants in the activation pathway so that it is slow relative to the other rate constants at −40 mV and equal to or faster than them at 0 mV. As

discussed earlier, this highly voltage-dependent transition is not likely to be either the first or the last transition in the activation pathway. (*b*) Alternatively, a single or small number of transitions could become rate limiting because the state immediately before the transition rapidly reaches a very low steady state probability of occupancy. The activation rate is then determined by the low probability of being in this closed state(s) times the rate constant for the transition.

A slow apparent closing transition, like that described earlier, would produce the relatively rapid equilibration among the closed states at hyperpolarized voltages, as proposed in the second mechanism. The voltage dependence of the sigmoidicity can be accounted for by a modification of Scheme V where the rate constant for the first closing transition is slowed relative to the rate constants for the other reverse transitions, as summarized by the following scheme:

$$C_1 \underset{\beta}{\overset{n\alpha}{\leftrightarrow}} C_2 \underset{2\beta}{\overset{(n-1)\alpha}{\longleftrightarrow}} \cdots \underset{(n-1)\beta}{\overset{2\alpha}{\longleftrightarrow}} C_n \underset{\frac{n\beta}{\theta}}{\overset{\alpha}{\longleftrightarrow}} O$$

SCHEME VI

where θ is the factor by which the first closing transition is slowed. The predictions of Scheme VI were calculated for $n = 8$ and $\theta = 10$ using the rate constants and voltage dependencies determined above. The predictions of the activation time courses are plotted in Fig. 13 *E*, and are normalized in Fig. 13 *F*. Scheme VI accurately reproduces the reduction in sigmoidicity at −40 and −50 mV relative to 0 and +50 mV. Note also that in both the data and in the model there is almost no difference in sigmoidicity between 0 and +50 mV even though the activation is nearly three times faster at +50 mV. As shown in Fig. 14 the sigmoidicity is unchanged up to at least +100 mV. This reflects the fact that in the model the forward rate constants have identical voltage dependencies, and therefore the relative amplitude of the forward rate constants remains unchanged at different voltages. Because at these depolarized voltages the reverse rate constants are effectively zero, the relative amplitude of the forward rate constants is the sole determinant of the degree of sigmoidicity. This reinforces the conclusion made earlier that many or perhaps all of the forward rate constants must have a similar voltage dependence. If one or a small number of transition rate constants were substantially less voltage dependent, they would become rate limiting at very depolarized voltages and cause a decrease in the sigmoidicity, which is not observed.

This slow apparent closing transition also manifests itself on the time course of reactivation after hyperpolarizing pulses. As shown earlier in Fig. 9, the time course of reactivation after brief hyperpolarizing pulses is well described by a single exponential function. However, after longer hyperpolarizing pulses the reactivation becomes appreciably sigmoidal. Fig. 15 *A* shows the time course of reactivation at +50 mV after hyperpolarizations of various durations to −70 mV. This reflects the fact that, when allowed to deactivate for longer periods of time, the channels progress to closed states more distant from the open state and therefore must undergo multiple transitions before reopening (Oxford, 1981). A mechanism with any number of independent transitions would predict that reactivation curves should all follow the

time course of normal activation after a simple shift along the time axis. This prediction is exactly analogous to that of Cole and Moore (Cole and Moore, 1960) for the effect of holding voltage on the time course of activation. Fig. 15, *B* and *C*, shows the results of shifting the reactivation curves, after hyperpolarizations to −70 and −90 mV, respectively, along the time axis to equate the final phases of their time courses. Note that, unlike the predictions of an independent scheme, the currents become appreciably sigmoidal well before deactivation is complete. This observation can be explained by a mechanism where the channels, after closing, rapidly progress

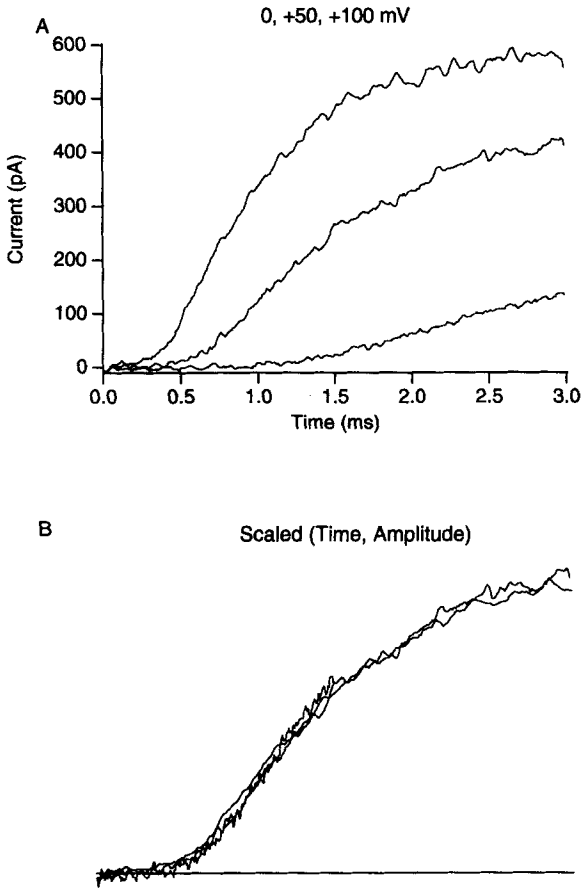

FIGURE 14. Activation kinetics and sigmoidicity at very depolarized voltages. (*A*) Macroscopic currents elicited by voltage steps to 0, +50, and +100 mV from a holding voltage of −90 mV. The data were filtered at 10 kHz and digitized every 10 μs. (*B*) The currents recorded at 0, +50, and +100 mV were scaled vertically and horizontally as described in the text and the legend for Fig. 13 to compare the sigmoidicity. The scaled currents superimpose.

to closed states more distant from the open state. Once again the deviations from the predictions of an independent gating scheme are consistent with a first closing transition that is slow relative to the other reverse transitions.

The rate of the reverse transitions distant from the open state can be investigated by analyzing the time course of the OFF gating currents at hyperpolarized voltages after depolarizing voltage steps. Because the gating currents measure the rate of occurrence of voltage-dependent transitions, they can be observed for channels that progress among the closed states in the activation pathway but have not yet opened.

Fig. 16 *A* shows the ionic and gating currents produced by variable length pulses to +50 mV followed by pulses to −100 mV. These ionic currents were recorded in the identical solutions as the gating currents except that the 140 mM NMG Cl in the internal solution was replaced by 140 mM KCl. At the end of the very short depolarizing pulse (1 ms) most of the channels had not yet opened as indicated by the small ionic current produced. Yet, the ON and OFF gating currents were quite

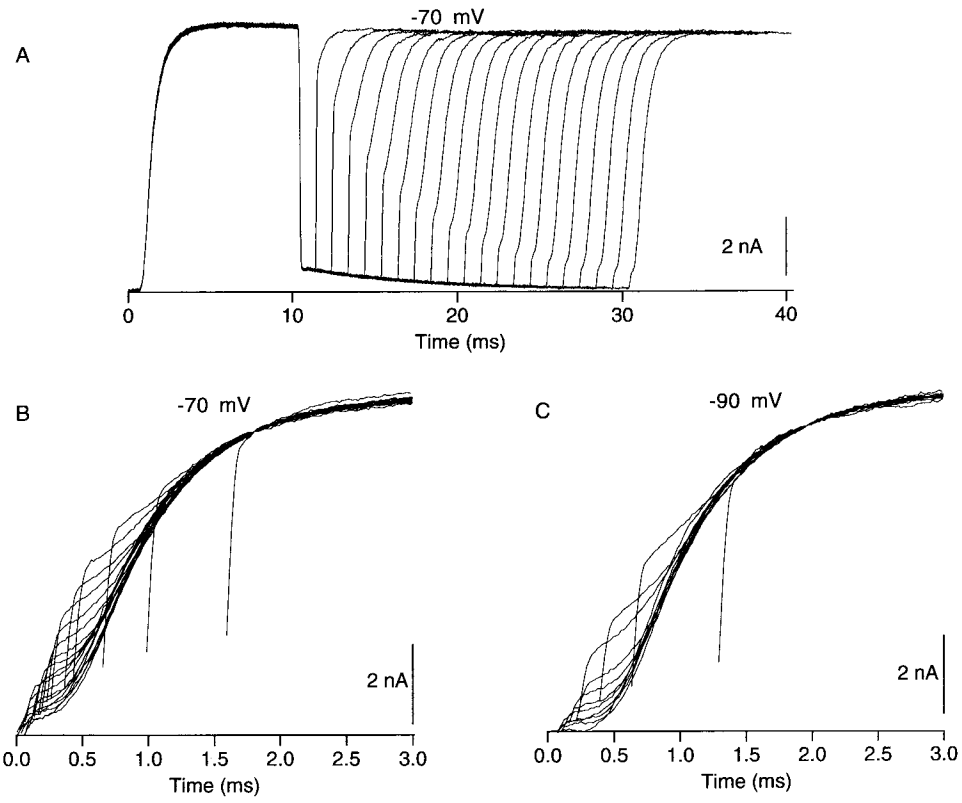

FIGURE 15. Time course of reactivation. (*A*) Two voltage pulses to +50 mV separated by repolarization to −70 mV for 1 to 20 ms were given. The data were filtered at 4 kHz and digitized every 20 μs. Note the change in the activation kinetics during the second pulse with the different interpulse durations. (*B*) The currents shown in A are shifted along the time axis to match the late phase of the activation to compare the redevelopment of the sigmoidal characteristic. (*C*) The currents were elicited as in *A* except that the interpulse voltage was −90 mV. The resulting currents were shifted along the time axis as in *B*.

large. This indicates that, during the depolarizing pulse, many of the channels had progressed among the closed states in the activation pathway but had not yet opened. These channels were able to return to their resting closed state quite rapidly as indicated by the large amplitude, rapid OFF gating current. The time constant of this rapid component of decay of the OFF gating currents after short pulses was about 0.5 ms at −100 mV. However, with longer depolarizing pulses where most of the

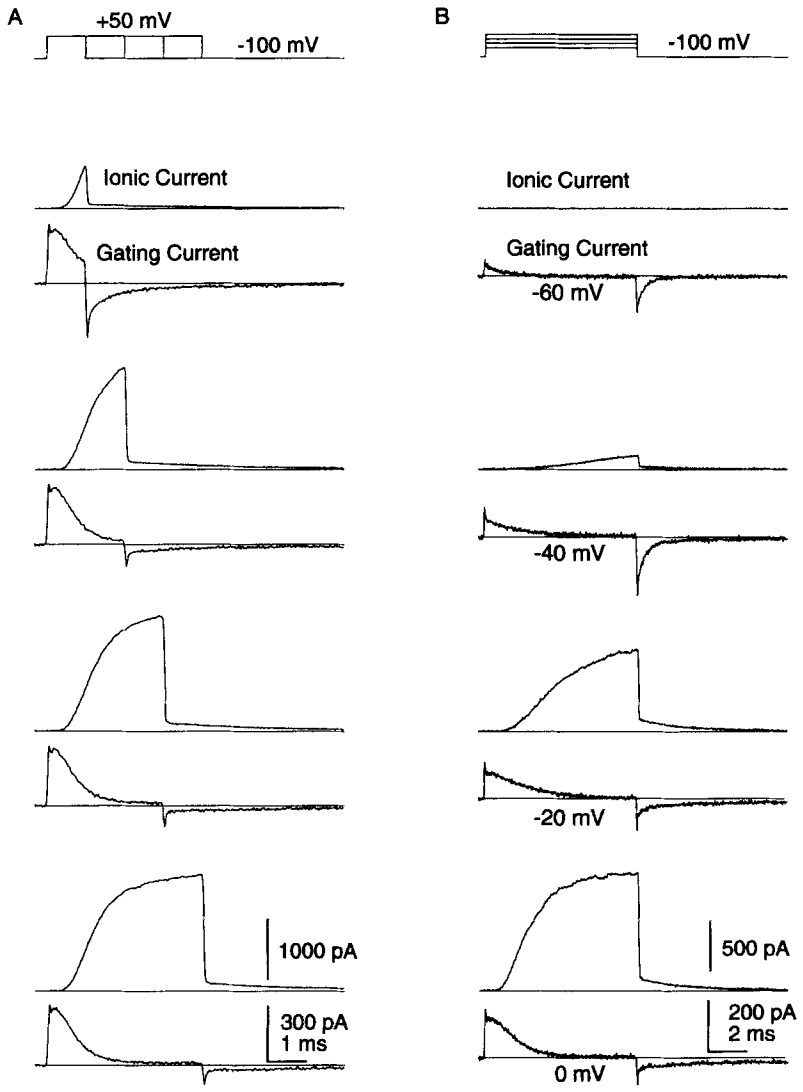

FIGURE 16. Comparison of gating charge movement and ionic current kinetics. (*A*) Ionic and gating currents were elicited in response to 8-ms voltage pulses to +50 mV for 1, 2, 3, and 4 ms from a holding voltage of −100 mV. The data were filtered at 8 kHz and digitized at 18 μs. The gating currents were recorded as described in Materials and Methods. The ionic currents were recorded with the K^+-free NMG extracellular solution used to record the gating currents and with the standard K^+-containing intracellular solution. The ionic and gating currents were recorded from different patches. (*B*) The ionic and gating currents were recorded in response to voltage pulses to −60, −40, −20, and 0 mV from a holding voltage of −100 mV. The data were filtered at 8 kHz and digitized every 16 μs. The ionic currents were recorded as in *A*.

channels reached the open state, the OFF gating currents were much smaller and slower. Similar results have been reported for the gating currents of RBK1 and *Shaker* potassium channels (Stuhmer et al., 1991). A similar effect to that described above occurs with variable amplitude depolarizing pulses. Fig. 16 *B* shows the ionic and gating currents produced by an 8 ms depolarizing pulse to between −60 and 0 mV followed by a pulse to −100 mV. Note that the depolarizing pulses below −20 mV are associated with rapid, large amplitude OFF gating currents while the depolarizing pulses above −20 mV are followed by a much smaller and slower OFF gating current. The time course of the OFF gating current after a pulse to −40 mV is very similar to that after a 1 ms pulse to +50 mV. Once again the small, slow gating currents occur when the depolarizing pulse opens a substantial fraction of the channels. Note that in an activation scheme involving identical and independent conformational changes there would be no dependence of the OFF gating current time course on the amplitude or duration of the depolarizing pulse. These results indicate that, upon hyperpolarization, an open channel returns much more slowly to its resting state than does a not-yet opened channel, suggesting a slow first closing transition.

In contrast to the OFF gating currents, the time course of the tail currents does not depend on the duration of the depolarizing pulse. The tail currents in Fig. 16 *A*, after 1 to 4 ms depolarizing pulses, were normalized and superimposed in Fig. 17 *A*. The similarity in the time course of these tail currents is consistent with a mechanism where the channel enters only a single open state during steps to +50 mV. It should be noted that the rate of deactivation in these modified gating current solutions is somewhat slower than that in normal solutions. In normal solutions the time constant of deactivation at −100 mV is about 1 ms (see Fig. 11 *C*) while in these solutions the time constant is ~3 ms (see the single-exponential fit superimposed on the data in Fig. 17 *A*). The difference in deactivation rates appears to be due to the replacement of 140 mM NaCl and 2 mM KCl in the normal solutions with 142 mM NMG Cl in the modified gating current solutions. This effect was not investigated further.

If the rate constant for the first closing transition is markedly slower than the rate constants of the other reverse transitions, it should represent the rate limiting step for both channel closure and return of gating charge. The time course of these two events is directly compared in Fig. 17 *B* by overlaying the tail currents and the OFF gating currents from Fig. 16 *A*. As expected, with short depolarizing pulses the OFF gating currents are considerably faster than the tail currents, because most of the gating currents are arising from channels that have not yet opened. However, with longer depolarizing pulses, the OFF gating currents and the tail current nearly superimpose. This similarity in the time course of the gating currents has also been observed by Bezanilla et al. (Bezanilla et al., 1991). An activation scheme involving n identical and independent conformational changes would predict that the tail currents at hyperpolarized voltages would be n times faster than the OFF gating currents (Armstrong, 1981; Armstrong and Bezanilla, 1974; Rojas and Keynes, 1975), clearly not observed here. Instead, it appears that the same step is rate limiting for both processes, namely the first closing transition, as also seen in voltage-dependent sodium channels (Armstrong, 1981; Armstrong and Bezanilla, 1974; Rojas and Keynes, 1975).

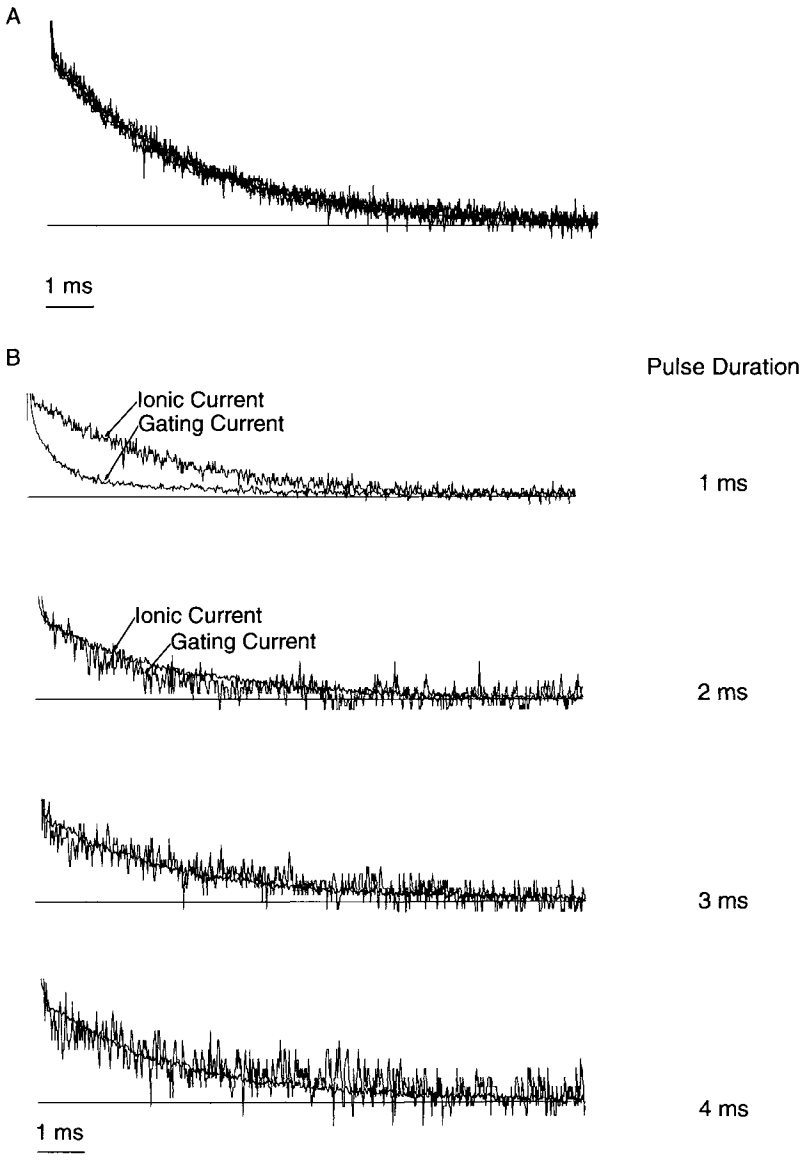

FIGURE 17. Ionic tail current and OFF gating current kinetics with different pulse durations. (*A*) The ionic tail currents recorded at −100 mV after depolarization to +50 mV for 1, 2, 3, and 4 ms were scaled so that their amplitudes are the same. The currents superimpose. The tail currents were recorded as described for Fig. 16. A single exponential curve with a time constant of 3 ms is also shown superimposed. (*B*) Comparison of the OFF gating currents and the tail currents recorded at −100 mV after depolarization to +50 mV for 1, 2, 3, and 4 ms. The OFF gating currents and the tail currents were scaled so that their apparent amplitudes immediately after the depolarizing were the same. After the 1 ms pulse, the gating current decays faster. For the remaining data sets, the noisiest of the two sweeps is the gating current.

DISCUSSION

In this paper we have identified four characteristics of the activation process that must be accounted for by any kinetic model for activation. (*a*) The activation conformational changes are associated with the movement of charge equivalent to 12 to 16 electronic charges through the membrane electric field. (*b*) Opening of the channel from hyperpolarized voltages requires at least five sequential conformation changes. (*c*) The total charge movement is spread out among many or all of these conformational changes and resides more in the reverse transitions than in the forward transitions. (*d*) The first closing transition is slower than expected for a model involving a number of independent and identical transitions. In the following paper we will consider a number of specific kinetic schemes to account for these characteristics. In this section we will discuss some precedents for these observations and their implications for the activation mechanism.

Large Amount of Charge Movement Associated with Activation Transitions

The estimate of 12 to 16 electronic charges is consistent with some previous measurements of charge movement in *Shaker* channels. Schoppa et al. (Schoppa et al., 1992) calculated a charge movement of 12.3 charges per channel from the integrated gating current and the estimated number of channels in the patch. The similarity of these estimates of charge movement is quite striking given the differences in the approach and assumptions involved. This charge movement is somewhat larger than an estimate for native *Shaker* channels (9.4 electronic charges) which relied largely on the voltage-dependence of the steady state inactivation and the coupling of activation and inactivation (Zagotta and Aldrich, 1990*b*). If the inactivation from closed states was somewhat larger than predicted, then the charge movement required to fit the steady state inactivation curve would have been larger. Finally, this charge movement is considerably larger than previous estimates in *Shaker* channels made from limiting slope measurements of the steady state P_o vs voltage data, which ranged between 4 and 9 charges (Iverson, Tanouye, Lester, Davidson, and Rudy, 1988; Papazian, Timpe, Jan, and Jan, 1991; Schoppa et al., 1992; Timpe, Jan, and Jan, 1988). This underscores the need to measure extremely small open probabilities to obtain an accurate measurement of charge movement, as demonstrated in Fig. 2 *B*.

The high degree of charge movement in the activation process greatly constrains the possible conformational changes that might occur during activation. Because *Shaker* potassium channels exist as homotetramers in *Xenopus* oocytes (MacKinnon, 1991), it is generally believed that activation reflects, at least in part, four identical, although not necessarily independent, processes. Therefore, a total charge movement of 12 to 16 electronic charges would correspond to the equivalent of 3 to 4 charges moving through the entire membrane electric field for each subunit. In most voltage-dependent channels, this charge movement is thought to arise from the movement of the amphipathic S4 region in the membrane during the activation conformational changes (Catterall, 1986; Durell and Guy, 1992; Greenblatt, Blatt, and Montal, 1985; Guy and Seetharamulu, 1986; Liman, Hess, Weaver, and Koren, 1991; Lopez, Jan, and Jan, 1991; Noda, Ikeda, Suzuki, Takeshima, Takahashi, Kuno,

and Numa, 1986; Papazian et al., 1991; Schoppa et al., 1992; Stuhmer, Conti, Suzuki, Wang, Noda, Yahagi, Kubo, and Numa, 1989). The S4 region of *Shaker* channels contains seven positively charged amino acids spaced three residues apart, with intervening hydrophobic residues (Kamb, Tseng, and Tanouye, 1988; Pongs, Kecskemethy, Muller, Krah, Baumann, Kiltz, Canal, Llamazares, and Ferrus, 1988; Tempel, Papazian, Schwarz, Jan, and Jan, 1987). To move the equivalent of three electronic charges through the membrane, this structure would have to move a very large distance orthogonal to the membrane during the conformational change(s). Alternatively, there could be considerable charge movement occurring elsewhere in the channel protein that contributes to the total charge movement.

More Than Five Transitions Before Opening

The high degree of sigmoidicity associated with activation indicates that the activation process requires more than five sequential conformation changes. Other investigators have also found that four transitions is not adequate to describe the sigmoidal delay. Hodgkin and Huxley (Hodgkin and Huxley, 1952) described the activation kinetics of the squid voltage-dependent potassium channel with four independent and identical gating particles but commented that six gating particles would be more accurate, but for their purposes was computationally impractical. Gilly and Armstrong (1982) came to a similar conclusion. Cole and Moore (1960) found that they needed 25 independent and identical gating transitions to reproduce the sigmoidal delay in the squid potassium channel when activated from very hyperpolarized voltages. The requirement for more than four sequential transition before opening indicates that activation must involve more than just one conformational change in each of its subunits. The suggestion of additional types of conformational changes was also made by Schoppa et al. (1992) who have shown that mutations in the S4 segment separate the gating current into two components. These data suggest two types of voltage-dependent conformational changes, both of which are required for opening. The additional voltage-dependent transitions could arise from either multiple conformational changes per subunit or from multiple concerted conformational changes. In the following paper (Zagotta et al., 1994), we will demonstrate that a model involving two voltage-dependent conformational changes per subunit can account for all of the characteristics of the activation process described here.

Charge Movement Is Spread Out Among Many of the Transitions

Based on the similarity in sigmoidicity between 0 and +100 mV, we have proposed that the rate constants of many or perhaps all of the forward conformational changes have a similar voltage dependence. If one or more of the forward transitions were voltage independent and not exceedingly rapid, as in the model of Zagotta and Aldrich (1990*b*), then it would become rate limiting for activation at extremely depolarized voltages, greatly reducing the sigmoidicity. Schoppa et al. (Schoppa, McCormack, Tanouye, and Sigworth, 1991) showed that the *Shaker* currents continue to become more rapid and maintain a substantial delay even at extremely depolarized voltages. In the previous paper (Hoshi et al., 1994), we have shown that the channel can rapidly reopen from a closed state *Cf* with a rate constant that does not depend on voltage. If the $Cf \rightarrow O$ transition is completely voltage-independent, it

cannot be a part of the normal activation pathway. Taken together with the conclusion of the previous paper that the $O \rightarrow Cf$ transition can not be a part of the normal deactivation pathway, these results suggest that the Cf state can only be entered after opening. However, because the rate of the forward transitions exhibit only a small amount of voltage dependence, we cannot rule out possibility that the rate of the $O \rightarrow Cf$ transition exhibits a small voltage dependence that prevents it from becoming rate limiting.

Departures from Independent and Identical Transitions

Cole and Moore (Cole and Moore, 1960) showed that, at more depolarized holding voltages, the sigmoidal delay is decreased as if the channels must undergo fewer transitions before opening. Furthermore, if the currents were shifted along the time axis by an amount equal to the lost delay, the activation at different holding voltages followed a similar time course. As shown in Fig. 5, this result also holds for *Shaker* channels at holding voltages below −60 mV and suggests that the activation of the channels involves the independent action of a number of transitions, such as conformational changes in each subunit. Hill and Chen (1971*a*,*b*) showed that if the conformational changes in each subunit are not independent, but instead exhibited significant cooperative interactions, the activation time courses from different holding voltages would no longer be similar. The departure of the *Shaker* channels from this Cole-Moore effect occurs with holding voltages above −60 mV, where there is an appreciable steady state probability of being in the open state. This departure is consistent with a first closing transition that is slower than expected for an activation process involving a number of independent and identical transitions.

Other investigators have also found that the kinetics of activation in voltage-dependent potassium channels departs from the expectations of multiple independent and identical transitions. Gilly and Armstrong (1982) suggested that there was a slow step in the activation process of squid potassium channels on the basis of poor fits of independent models to the macroscopic activation time course. Furthermore, they suggested that the last step was not rate limiting based on the time course of reactivation with short hyperpolarizing pulses. As shown in Fig. 4, the activation time course in *Shaker* channels is quite reasonably described by multiple independent and identical transitions. The gating currents from squid potassium channels depart quite markedly from the predictions of multiple independent and identical transitions (Gilly and Armstrong, 1980; White and Bezanilla, 1985). The ON gating currents exhibited a rising phase instead of following a single-exponential time course, and the OFF gating currents had a similar time course as the tail currents instead of being four times slower. Both of these phenomena were seen in the *Shaker* potassium channels and can be accounted for by the model described in the following paper.

Many mutations have been found in the S4 segment, the S4-S5 linker, and the S5 segment that profoundly alter the voltage-dependent activation process (Gautam and Tanouye, 1990; Lichtinghagen, Stocker, Wittka, Boheim, Stuhmer, Ferrus, and Pongs, 1990; Liman et al., 1991; Lopez et al., 1991; McCormack, Tanouye, Iverson, Lin, Ramaswami, McCormack, Campanelli, Mathew, and Rudy, 1991; Papazian et al., 1991; Schoppa et al., 1992; Stuhmer et al., 1989; Zagotta and Aldrich, 1990*a*). The interaction between subunits has been explored by examining some of these

mutations in heteromultimeric channels, containing the mutation in only some of their subunits (Hurst, Kavanaugh, Yakel, Adelman, and North, 1992; Tytgat and Hess, 1992). The steady state voltage dependence of the activation process in these heteromultimers was not as expected for independent subunits, but, instead, was consistent with cooperative interactions between subunits. Tytgat and Hess (Tytgat and Hess, 1992) modeled these cooperative interactions as a constant energy of stabilization for the activation conformational change of a subunit when a neighboring subunit is activated. A similar model for cooperative interactions has previously been shown to be inconsistent with the superposition of currents from different holding voltages shown by Cole and Moore (Cole and Moore, 1960) (Hill and Chen, 1971*a*,*b*). However this model may be consistent with the small deviations shown in Fig. 5. As shown in the following paper, a slow first closing transition will appear, in many ways, as a form of cooperativity. In particular, a model with a slow first closing transition can quantitatively account for the voltage-dependence of activation in heteromultimers as well as the results of the Cole-Moore experiment in Fig. 5.

The apparent slow first closing transition also exerts a number of other effects on the steady state and kinetic properties of the channel. (*a*) The tail current time course is slowed. (*b*) The sigmoidicity in the activation time course is decreased at hyperpolarized voltages. (*c*) The reactivation time course becomes sigmoidal before deactivation is complete. (*d*) The OFF gating currents are larger and more rapid after short or low amplitude voltage pulses where the channels have not been allowed to reach the open state. (*e*) The time course of the tail currents and the OFF gating currents from channels in the open state are similar. (*f*) And, as shown in the following paper (Zagotta et al., 1993), the steady-state P_o vs voltage curve becomes steeper at intermediate and high probabilities.

The apparent slow first closing transition strongly suggest that channel closure does not come about just by the reverse transition of one of a number of independent and identical conformational changes. While the closed states *Cf* and *Ci*, described in the previous paper (Hoshi et al., 1994), will have some effects on the kinetics of deactivation, they cannot account for the observed slowing of the first closing transition. This apparent slowing could arise from a number of different mechanisms. The first closing transition could represent a fundamentally different type of conformational change from the others that occur during the activation process, such as a concerted conformational change that occurs after a number of independent and identical transitions (Koren, Liman, Logothetis, Nadal, and Hess, 1990; Zagotta and Aldrich, 1990*b*). Alternatively the closing transition could represent the same type of conformational change but occurs at a slower rate due to a stabilization of the open state by hydration effects or cooperative interactions. A third possibility is that the deactivation time course of the channel could be slow not because of an intrinsically slow closing conformational change, but because the channel cannot close with ions in the pore, a mechanism that has been called the occupancy hypothesis (Ascher et al., 1978; Marchais and Marty, 1979; Matteson and Swenson, 1986; Swenson and Armstrong, 1981). Because potassium channels are generally thought to possess multi-ion pores, the open channel probably spends a large fraction of its time with an ion in the pore. This would greatly reduce the amount of time available for the channel to close and thereby produce slow deactivation. In other voltage-dependent

potassium channels this mechanism has been proposed to account for the slowing of deactivation in the presence of various external monovalents (Cahalan et al., 1985; Matteson and Swenson, 1986; Sala and Matteson, 1991; Shapiro and DeCoursey, 1991*a,b;* Spruce et al., 1989; Swenson and Armstrong, 1981).

Consistent with the occupancy hypothesis, small differences in the ionic conditions can make large differences in the macroscopic deactivation rate. The presence of Rb^+ in the external solution causes a slowing of deactivation (Fig. 12). The voltage dependence of the tail current time course was not appreciably altered in Rb^+ suggesting that the Rb^+ occupancy is not particularly voltage dependent. This is similar to what has been observed for squid voltage-dependent potassium channels (Matteson and Swenson, 1986) but different from that observed for voltage-dependent potassium channels from toadfish pancreatic islet cells (Sala and Matteson, 1991). In addition, we have shown that the tail currents were nearly threefold slower when the external solution has 142 mM NMG Cl replacing the 140 mM NaCl and 2 mM KCl present in our standard solutions. This threefold slowing of the deactivation rate causes a much smaller and slower OFF gating current. Furthermore, it suggests that the lack of K^+ or Na^+ or the presence of NMG^+ in the external solution results in a slower first closing transition.

The OFF gating currents reported by other investigators have varied considerably with the composition of the solutions and the method used for subtracting linear capacitance. For *Shaker* channels that have reached the open state, the OFF gating currents have ranged from very slow, low amplitude currents to transient, moderate amplitude currents with a clearly discernible rising phase (Bezanilla et al., 1991; Perozo et al., 1992; Schoppa et al., 1992; Stuhmer et al., 1991). This range of behavior can be reproduced by varying only the rate constant for the first closing transition. With slow first closing transitions, the OFF gating currents are quite small and slow. This behavior is similar to that reported for some potassium channels by Stuhmer et al. (Stuhmer et al., 1991). Small and slow OFF gating currents are also seen when tetraethyl ammonium (TEA) is used in the internal solutions which greatly slows the deactivation rate (Bezanilla et al., 1991). With faster first closing transitions, the OFF gating currents are large and transient, similar to those reported by Bezanilla et al. (Bezanilla et al., 1991).

We thank Tom Middendorf and Max Kanevsky for helpful comments on the manuscript, and Ted Begenisich for help with our initial gating current experiments.

This work was supported by a grant from National Institutes of Health (NS23294) and by a National Institute of Mental Health Silvio Conte Center for Neuroscience Research Grant (MH 48108). W. N. Zagotta is a Warner-Lambert fellow of the Life Sciences Research Foundation. R. W. Aldrich is an investigator with the Howard Hughes Medical Institute.

Original version received 13 May 1993 and accepted version received 27 August 1993.

REFERENCES

Almers, W. 1978. Gating currents and charge movements in excitable membranes. *Review Physiology and Biochemical Pharmacology.* 82:96–190.

Andersen, O. S., and R. E. Koeppe. 1992. Molecular determinants of channel function. *Physiological Reviews.* 72:89–158.

Armstrong, C. M. 1981. Sodium channels and gating currents. *Physiological Reviews.* 61:644–683.

Armstrong, C. M., and F. Bezanilla. 1974. Charge movement associated with the opening and closing of the activation gates of the Na channels. *Journal of General Physiology.* 63:533–552.

Ascher, P., A. Marty, and T. O. Neild. 1978. Life time and elementary conductance of the channels mediating the excitatory effects of acetylcholine in Aplysia neurones. *Journal of Physiology.* 278:177–206.

Bezanilla, F., E. Perozo, D. M. Papazian, and E. Stefani. 1991. Molecular basis of gating charge immobilization in *Shaker* potassium channels. *Science.* 254:679–683.

Cahalan, M. D., K. G. Chandy, T. E. DeCoursey, and S. Gupta. 1985. A voltage-gated potassium channel in human T lymphocytes. *Journal of Physiology.* 358:197–237.

Catterall, W. A. 1986. Molecular properties of voltage-sensitive sodium channels. *Annual Review of Biochemistry.* 55:953–985.

Cole, K. S., and J. W. Moore. 1960. Potassium ion current in the squid giant axon: dynamic characteristic. *Biophysical Journal.* 1:1–14.

Durell, S. R., and H. R. Guy. 1992. Atomic scale structure and functional models of voltage-gated potassium channels. *Biophysical Journal.* 62:238–250.

Gautam, M., and M. A. Tanouye. 1990. Alteration of potassium channel gating: molecular analysis of the *Drosophila* Sh5 mutation. *Neuron.* 5:67–73.

Gilly, W. F., and C. M. Armstrong. 1980. Gating current and potassium channels in the giant axon of the squid. *Biophysical Journal.* 29:485–492.

Gilly, W. F., and C. M. Armstrong. 1982. Divalent cations and the activation kinetics of potassium channels in squid giant axons. *Journal of General Physiology.* 79:965–996.

Greenblatt, R. E., Y. Blatt, and M. Montal. 1985. The structure of the voltage-sensitive sodium channel. Inferences derived from computer-aided analysis of the Electrophorus electricus channel primary structure. *FEBS Letters.* 193:125–134.

Guy, H. R., and P. Seetharamulu. 1986. Molecular model of the action potential sodium channel. *Proceedings of the National Academy of Sciences, USA.* 83:508–512.

Hill, T. L., and Y. D. Chen. 1971*a*. On the theory of ion transport across the nerve membrane. 3. Potassium ion kinetics and cooperativity (with x = 4,6,9). *Proceedings of the National Academy of Sciences, USA.* 68:2488–2492.

Hill, T. L., and Y. D. Chen. 1971*b*. On the theory of ion transport across the nerve membrane. II. Potassium ion kinetics and cooperativity (with x = 4). *Proceedings of the National Academy of Sciences, USA.* 68:1711–1715.

Hille, B. 1992. Ionic Channels of Excitable Membranes. Sinauer Associates Inc., Sunderland, MA. 607 pp.

Hodgkin, A. L., and A. F. Huxley. 1952. A quantitative description of membrane current and its application to conduction and excitation in nerve. *Journal of Physiology.* 117:500–544.

Hoshi, T., W. N. Zagotta, and R. W. Aldrich. 1994. *Shaker* potassium channel gating I: Transitions near the open state. *Journal of General Physiology.* 103:249–278.

Hurst, R. S., M. P. Kavanaugh, J. Yakel, J. P. Adelman, and R. A. North. 1992. Cooperative interactions among subunits of a voltage-dependent potassium channel. Evidence from expression of concatenated cDNAs. *Journal of Biological Chemistry.* 267:23742–23745.

Iverson, L. E., M. A. Tanouye, H. A. Lester, N. Davidson, and B. Rudy. 1988. A-type potassium channels expressed from *Shaker* locus cDNA. *Proceedings of the National Academy of Sciences, USA.* 85:5723–5727.

Kamb, A., C. J. Tseng, and M. A. Tanouye. 1988. Multiple products of the Drosophila *Shaker* gene may contribute to potassium channel diversity. *Neuron.* 1:421–430.

Koren, G., E. R. Liman, D. E. Logothetis, G. B. Nadal, and P. Hess. 1990. Gating mechanism of a cloned potassium channel expressed in frog oocytes and mammalian cells. *Neuron.* 4:39–51.

Lichtinghagen, R., M. Stocker, R. Wittka, G. Boheim, W. Stuhmer, A. Ferrus, and O. Pongs. 1990. Molecular basis of altered excitability in *Shaker* mutants of *Drosophila* melanogaster. *EMBO Journal.* 9:4399–4407.

Liman, E. R., P. Hess, F. Weaver, and G. Koren. 1991. Voltage-sensing residues in the S4 region of a mammalian K^+ channel. *Nature.* 353:752–756.

Liman, E. R., J. Tytgat, and P. Hess. 1992. Subunit stoichiometry of a mammalian K^+ channel determined by construction of multimeric cDNAs. *Neuron.* 9:861–871.

Lopez, G. A., Y. N. Jan, and L. Y. Jan. 1991. Hydrophobic substitution mutations in the S4 sequence alter voltage-dependent gating in *Shaker* K^+ channels. *Neuron.* 7:327–336.

MacKinnon, R. 1991. Determination of the subunit stoichiometry of a voltage-activated potassium channel. *Nature.* 350:232–235.

Marchais, D., and A. Marty. 1979. Interaction of permeant ions with channels activated by acetylcholine in Aplysia neurones. *Journal of Physiology.* 297:9–45.

Matteson, D. R., and R. J. Swenson. 1986. External monovalent cations that impede the closing of K channels. *Journal of General Physiology.* 87:795–816.

McCormack, K., M. A. Tanouye, L. E. Iverson, J. W. Lin, M. Ramaswami, T. McCormack, J. T. Campanelli, M. K. Mathew, and B. Rudy. 1991. A role for hydrophobic residues in the voltage-dependent gating of *Shaker* K^+ channels. *Proceedings of the National Academy of Sciences, USA.* 88:2931–2935.

Noda, M., T. Ikeda, H. Suzuki, H. Takeshima, T. Takahashi, M. Kuno, and S. Numa. 1986. Expression of functional sodium channels from cloned cDNA. *Nature.* 322:826–828.

Oxford, G. S. 1981. Some kinetic and steady-state properties of sodium channels after removal of inactivation. *Journal of General Physiology.* 77:1–22.

Papazian, D. M., L. C. Timpe, Y. N. Jan, and L. Y. Jan. 1991. Alteration of voltage-dependence of Shaker potassium channel by mutations in the S4 sequence. *Nature.* 349:305–310.

Perozo, E., D. M. Papazian, E. Stefani, and F. Bezanilla. 1992. Gating currents in *Shaker* K^+ channels. Implications for activation and inactivation models. *Biophysical Journal.* 62:160–168 171.

Pongs, O., N. Kecskemethy, R. Muller, J. I. Krah, A. Baumann, H. H. Kiltz, I. Canal, S. Llamazares, and A. Ferrus. 1988. *Shaker* encodes a family of putative potassium channel proteins in the nervous system of *Drosophila. EMBO Journal.* 7:1087–1096.

Rojas, E., and R. D. Keynes. 1975. On the relation between displacement currents and activation of the sodium conductance in the squid giant axon. *Philosophical Transactions of the Royal Society of London B.* 270:459–482.

Sala, S., and D. R. Matteson. 1991. Voltage-dependent slowing of K channel closing kinetics by Rb^+. *Journal of General Physiology.* 98:535–554.

Schoppa, N. E., K. McCormack, M. A. Tanouye, and F. J. Sigworth. 1991. High time-resolution recordings from oocytes injected with wild-type and V1 mutant *Shaker* 29-4 cDNAs. *Biophysical Journal.* 59:196*a*. (Abstr.)

Schoppa, N. E., K. McCormack, M. A. Tanouye, and F. J. Sigworth. 1992. The size of gating charge in wild-type and mutant *Shaker* potassium channels. *Science.* 255:1712–1715.

Shapiro, M. S., and T. E. DeCoursey. 1991*a*. Permeant ion effects on the gating kinetics of the type L potassium channel in mouse lymphocytes. *Journal of General Physiology.* 97:1251–1278.

Shapiro, M. S., and T. E. DeCoursey. 1991*b*. Selectivity and gating of the type L potassium channel in mouse lymphocytes. *Journal of General Physiology.* 97:1227–1250.

Spruce, A. E., N. B. Standen, and P. R. Stanfield. 1989. Rubidium ions and the gating of delayed rectifier potassium channels of frog skeletal muscle. *Journal of Physiology.* 411:597–610.

Stuhmer, W., F. Conti, M. Stocker, O. Pongs, and S. H. Heinemann. 1991. Gating currents of inactivating and noninactivating potassium channels expressed in *Xenopus* oocytes. *Pflügers Archiv.* 418:423–429.

Stuhmer, W., F. Conti, H. Suzuki, X. D. Wang, M. Noda, N. Yahagi, H. Kubo, and S. Numa. 1989. Structural parts involved in activation and inactivation of the sodium channel. *Nature.* 339:597–603.

Swenson, R. J., and C. M. Armstrong. 1981. K^+ channels close more slowly in the presence of external K^+ and Rb^+. *Nature.* 291:427–429.

Taglialatela, M., G. E. Kirsch, A. M. VanDongen, J. A. Drewe, H. A. Hartmann, R. H. Joho, E. Stefani, and A. M. Brown. 1992. Gating currents from a delayed rectifier K^+ channel with altered pore structure and function. *Biophysical Journal.* 62:34–36.

Taglialatela, M., L. Toro, and E. Stefani. 1992. Novel voltage clamp to record small, fast currents from ion channels expressed in *Xenopus* oocytes. *Biophysical Journal.* 61:78–82.

Taylor, R. E., and F. Bezanilla. 1983. Sodium and gating current time shifts resulting from changes in initial conditions. *Journal of General Physiology.* 81:773–784.

Tempel, B. L., D. M. Papazian, T. L. Schwarz, Y. N. Jan, and L. Y. Jan. 1987. Sequence of a probable potassium channel component encoded at *Shaker* locus of *Drosophila. Science.* 237:770–775.

Timpe, L. C., Y. N. Jan, and L. Y. Jan. 1988. Four cDNA clones from the *Shaker* locus of *Drosophila* induce kinetically distinct A-type potassium currents in *Xenopus* oocytes. *Neuron.* 1:659–667.

Tytgat, J., and P. Hess. 1992. Evidence for cooperative interactions in potassium channel gating. *Nature.* 359:420–423.

Vandenberg, C. A., and F. Bezanilla. 1991. A sodium channel gating model based on single channel, macroscopic ionic, and gating currents in the squid giant axon. *Biophysical Journal.* 60:1511–1533.

White, M. M., and F. Bezanilla. 1985. Activation of squid axon K^+ channels. Ionic and gating current studies. *Journal of General Physiology.* 85:539–554.

Zagotta, W. N., and R. W. Aldrich. 1990*a*. Alterations in activation gating of single *Shaker* A-type potassium channels by the Sh5 mutation. *Journal of Neuroscience.* 10:1799–1810.

Zagotta, W. N., and R. W. Aldrich. 1990*b*. Voltage-dependent gating of *Shaker* A-type potassium channels in *Drosophila* muscle. *Journal of General Physiology.* 95:29–60.

Zagotta, W. N., T. Hoshi, and R. W. Aldrich. 1994. Shaker potassium channel gating III: Evaluation of kinetic models for activation. *Journal of General Physiology.* 103:321–362.